



UNIVERSITÀ DEGLI STUDI DI MILANO

SCUOLA DI DOTTORATO  
*INFORMATICA*

DIPARTIMENTO  
*DI INFORMATICA "GIOVANNI DEGLI ANTONI"*

TESI DI DOTTORATO DI RICERCA

ARTIFICIAL INTELLIGENCE  
APPLIED TO THE STUDY  
OF CONSCIOUS PERCEPTIVE STATES

Marialessia Musumeci

TUTOR  
Prof.ssa Rita Pizzi

COORDINATORE DEL DOTTORATO  
Prof. Paolo Boldi

A.A.2018-2019



*To my husband*

## INDEX

<b>ABSTRACT</b>	<b>3</b>
<b>1 THE CONCEPT OF CONSCIOUSNESS IN NEUROSCIENCE</b>	<b>5</b>
<b>1.1 INTRODUCTION</b>	<b>5</b>
<b>1.2 INTEGRATED INFORMATION THEORY</b>	<b>8</b>
<b>1.3 THESIS OBJECTIVE</b>	<b>12</b>
<b>2 BRAIN AS DYNAMICAL SYSTEM</b>	<b>14</b>
<b>2.1 SELF-ORGANIZATION, COMPLEX SYSTEMS AND CHAOS</b>	<b>14</b>
<b>2.2 COMPLEXITY AND NON-LINEARITY</b>	<b>16</b>
<b>2.3 NON-LINEARITY AND DYNAMICAL SYSTEMS</b>	<b>17</b>
2.3.1 Non-Linear Analytical Methods	19
2.3.2 Fractal Dimension and Correlation Dimension	20
<b>2.4 ARTIFICIAL NEURAL NETWORKS AS DYNAMICAL SYSTEMS</b>	<b>24</b>
2.4.1 Stability and Regions of Attraction in Neural Models	24
2.4.2 Cohen-Grossberg THEOREM	26
2.4.3 Neural Models of Dynamical Systems Processing: Spatiotemporal Patterns in Artificial Neural Networks	31
2.4.4 Neural Models of Dynamical Systems Processing: Recurrent Neural Networks	33
2.4.5 Self-Organizing Networks	37
2.4.6 The ITSOM Architecture	40
2.4.7 Dynamical Analysis of ITSOM	44
2.4.8 Non-Linear Analysis of Cortical Signals and Functional Binding of Perceptions	46
<b>3 THE EXPERIMENTAL PHASE</b>	<b>51</b>
<b>3.1 EMOTIV EPOC +</b>	<b>51</b>
<b>3.2 EMOTIV EPOC + SOFTWARE: TEST BENCH</b>	<b>52</b>
<b>3.3 EMOTIV EPOC + 3D BRAIN ACTIVITY MAP</b>	<b>55</b>
<b>3.4 EPOC-SIMULINK CONNECTION</b>	<b>56</b>
<b>3.5 3D EXCELVAN GLASSES</b>	<b>59</b>
<b>3.6 SELECTED ELECTRODES</b>	<b>60</b>

<b>3.7 VIDEOS</b>	65
3.7.1 First Colors Test	65
3.7.2 Second Colors test	67
<b>3.8 EXPERIMENTAL PROCEDURE</b>	69
<b>4 SIGNAL PROCESSING</b>	71
<b>4.1 EMOTIVE EPOC +: DATA PRE-PROCESSING</b>	71
<b>4.2 PROCESSING</b>	72
<b>4.3 ITSOM APPLICATION</b>	74
4.3.1 ITSOM results	79
4.3.2 First Colors Test results	79
4.3.3 Second Colors Test results	81
<b>4.4 CORRESPONDENCE BETWEEN STIMULI AND         SHAPE OF ATTRACTORS</b>	84
<b>4.5 FINAL RESULTS</b>	88
<b>5 EVALUATION OF INTEGRATED INFORMATION</b>	90
<b>5.1 INTEGRATED INFORMATION CALCULUS</b>	94
<b>6 CONCLUSION</b>	99
<b>REFERENCES</b>	103
<b>INDEX OF FIGURES</b>	108
<b>INDEX OF TABLES</b>	109

## ABSTRACT

My PhD research consists of the processing of signals from a 14-electrode EEG system, connected to immersive glasses that allow for a realistic visual experience and for the investigation of the brain network in order to identify signal features corresponding to different perceptive and cognitive stimuli.

The aim of the research is to implement a procedure that identifies correspondences among EEG signals and chaotic attractors.

The chaotic attractors can be defined as a trajectory of a dynamical system, contained in a defined volume of phase space. A dynamical system can have chaotic behavior, i.e. an organized (but not periodic) behavior sensitive to the initial conditions. EEG signals can be considered dynamical systems.

In this work a custom Artificial Neural Network (ITSOM) processes individual signals or many signals simultaneously.

The sequence of the ITSOM winning nodes tends to repeat itself creating a time series of chaotic attractors.

The ITSOM attributes similar codes to attractors emerging from similar brain states, perceptions and emotions.

These attractors are isomorphic to the attractors in which the corresponding dynamical system (the signal time series) is evolving and univocally characterize the input element that produces them.

If the attractors are chaotic, this means that the signals are individually self-organized or, by examining more signals together, there is a form of coherence among signals.

The ITSOM network memorizes the time series of the winning nodes.

The cumulative scores for each input are normalized following the z standardized variable distribution.

Attractors are labeled with a binary code that univocally identifies them, and the flexibility of the Artificial Neural Network allows attributing the same codes to similar dynamical events.

During the experiment, the subject is looking at the screen while different shades of colors, yellow, red and blue are displayed. Each stimulation lasts five seconds, between stimuli there is a black screen, used to reset the previous color stimuli.

The collected results show, as forecast, many correspondences among binary codes coming from similar stimuli. The thesis provides a detailed description of these results.

# 1 THE CONCEPT OF CONSCIOUSNESS IN NEUROSCIENCE

## 1.1 INTRODUCTION

In the last decade, neurosciences have started to consider the concept of consciousness as a research subject, the definition and analysis of which constitutes one of the most fascinating and difficult challenges in modern science.

Various authors have attempted to describe the general properties of consciousness. Among them, Nagel [1], James [2], Greenfield [3], Hofstadter [4], Baars [5], Searle [6], Chalmers [7], Dennet [8], Metzinger [9], Baars [10].

Specifically, in 1948, the noted neurophysiologist, Charles S. Sherrington, in an article titled “The Integrative Action of the Nervous System” [11] wrote:

*“Every day of wakefulness is a stage dominated, for better or for worse, be it comedy, farce, or tragedy, by a personal drama, the "I". And so it will be until the curtain comes down. And this “I” is a unit. Its continuity in time, is only interrupted by sleep, its inalienable “interiority,” its stability of perspective, the private, subjective nature of its experience, combine to guarantee it a unique existence. Although characterized by multiple aspects, it has an internal cohesion.”*

In summary, Sherrington highlights two aspects of the “Ego” by analyzing three fundamental points:

1. Subjectivity: the state of the ego intended as the degree/level of personal impression;
2. Integration: the concept of conscious experience and its connections affirming "this ego is a unit". The problem of the feasibility in establishing a consciousness



3. measurement unit is not new: in philosophy at the times of Kant it was defined as the problem of the "transcendental unity of perception". Today, in neurophysiology the "binding problem" is discussed, i.e. the problem of how it is possible to "integrate" the activity of different and distant neuronal groups, under the assumption that their activity corresponds to different aspects of our conscious experience.
4. Informativity: the conscious experience is defined as the amount of information generated by the brain over a period of time, which unit of measurement is evaluated.

The examination of these three fundamental aspects of the human psyche has been interpreted from time to time, often in very different terms, by philosophers, psychologists of various backgrounds, psychiatrists interested in psychopathology, and finally by neurobiologists, who generally have tried to relate these to activity in certain areas of the brain. Depending on the branch of Neuroscience considered, the concept of consciousness assumes different meanings.

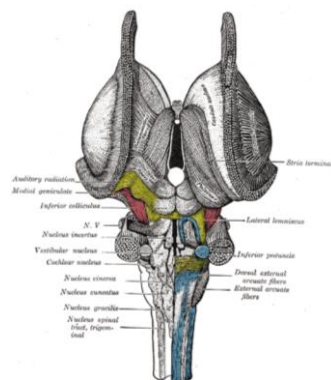
Some most neurobiological theories about consciousness assume that cortical activity as well as that of the thalamus provide a large part of the content of consciousness. The majority of these theories stems from the premise that the neural system that represents consciousness is a functional complex of neuronal cells, but it is not yet clear what neurons, cortical regions, or connections are involved.

Over the last fifteen years, Giulio Tononi has formulated a theoretical proposal to define consciousness and to provide an explanation on both why the thalamo-cortical system (Fig.1-1), unlike other structures such as the cerebellum, is more involved in conscious

experience, and why the different functional regime that involves this structure is able to determine the presence or absence of consciousness in different states of wakefulness and sleep. This is the Integrated Information Theory. The theory is founded on three fundamental principles:

1. Consciousness is born out of the rapid integration of a great quantity of information inside a dynamical nucleus of strongly integrated elements;
2. The reciprocal interconnections among the regions of the thalamocortical system mediate this rapid integration;
3. The onset of the “primary consciousness”, i.e., the construction of our multi-mode perceptual world, depends on the integration of sensory elaborations with the memory of previously gained experiences.

This theory highlights the importance of a complex integration of thalamocortical subsystems that appear to be functionally separated, yet highly interactive.



*Figure 1-1 Composition of the thalamocortical system. These structures transmit information both as inputs and output from the external environment, integrating their signals. Source: Anastasi, Motta, Balboni "Trattato di Anatomia Umana", Edi-Ermes, ed. IV, 2006.*

## 1.2 INTEGRATED INFORMATION THEORY

The Integrated Information Theory (IIT) [12] [13] [14] [15] [16] aims at explaining what consciousness is, by describing the requirements of the physical systems that make it possible and by measuring its quantity and quality thereof. Instead of starting from how the brain is structured or from the functions it performs, IIT reverses the question, going from phenomenology to physics: it begins by identifying the essential properties of consciousness itself to derive the necessary and sufficient requirements for why a physical substrate makes subjective experience possible. In summary, the Integrated Information Theory deals with the fundamental problem of consciousness: what are the necessary and sufficient conditions in which a physical system has the experience of consciousness?

The theory starts from two observations concerning the fundamental properties of the experience of consciousness: first of all, consciousness is highly informative; in fact, whenever we enter a particular conscious state (for example, when we see a dark blue sky), we exclude a number of possible alternative states (seeing red, yellow, darkness, rain, being in a room, being in a cinema and seeing a particular frame of one of all possible films, etc.). Secondly, consciousness is integrated; in fact, every conscious experience is absolutely unitary, we could never, for example, be separately conscious of the left or right visual field<sup>1</sup>. This fundamental statement can be derived from those two premises: "a physical system is conscious to the extent that it is able to integrate information". That is, the substrate of consciousness must be a system composed of many

---

<sup>1</sup> Actually this statement may be just a Tononi's assumption, as it is contradicted by the so-called "binocular rivalry" phenomenon: see e.g. *Baer N., and Baer W. "Interest-Attention Feedback System for Separating Cognitive Awareness in to Different Left and Right Sensor Display" Patent Application, 13/455,134, Filed 4/25/2012.*

functionally different elements (information) that are, however, closely linked to each other, forming an indivisible whole (integration). This is anything but trivial: it is a very delicate balance between diversity and unity.

This interpretation helps to solve many paradoxes concerning the brain-consciousness relationship. For example, it explains why an injury to the thalamo-cortical system can result in coma while the complete removal of the cerebellum (a very complicated structure with even more neurons) has no effect on consciousness. While the former is made up of elements functionally very different from each other but closely linked by short and long-distance nerve fibers, the latter has an essentially modular structure, not integrated. Similarly, this theory explains why consciousness is reduced during slow-wave sleep, even if the brain stays very active.

There are five essential properties of consciousness of every conceivable experience:

1. Its experience exists intrinsically (for the subject, not for an external observer);
2. It is structured (it is composed of various contents and their relationships);
3. It is informative (each experience is specific that which it is, therefore different from countless others);
4. It is integrated, in the sense discussed below;
5. It is well defined in the subjective experience.

These five essential properties of phenomenology are converted by IIT into the five physical requirements that must be satisfied by any physical substrate of consciousness, where "physical" means, very generally, any substrate that has causal power - that is, it can be directly or indirectly manipulated or observed - from the brain to neurons to elemental particles.

Tononi intuitively identifies a fundamental difference between a non-conscious system like a photodiode and a conscious system like Galileo, a human being. To describe this difference in scrupulous, mathematical and quantitative terms, Tononi refers to the mathematical information theory proposed by Claude Shannon and Warren Weaver [17].

According to the definitions given by the two two authors, the concept of information is based on that of entropy (H), i.e. the measure of the amount of "uncertainty" present in an aleatory signal. The concept of entropy, and therefore of uncertainty, emerges clearly using some representative examples taken from the theory of probability.

If entropy corresponds to uncertainty, information is classically defined as a measure of "reduction of uncertainty": the greater the number of alternative events excluded from the realization of the observed event, the greater the information brought by the event in question. In mathematical terms, the bit measurement of the amount of information associated with an event corresponds to the negative logarithm to the base two of the probability (P) of the event in question, or:

$$I(x) = -\log_2(P(x))$$

Another way of calculating the amount of information for each state, in fact, is to consider the number of possible states of a system, its repertoire of possible states (R), and to calculate the logarithm to the base two of that number. Given that each state has the same probability of being realized, the number of possible states will be equal to the reciprocal of the probability of realization of each single state.

The key to calculating the first fundamental difference in the information present in a system is suggested by analyzing not only the "observed" responses produced in output, but the "possible" responses.

Considering that the photodiode has a "binary" sensor capable of determining the presence or absence of light, it will have a repertoire of only two possible states, each corresponding to 1 bit of information. On the contrary, a human being like Galileo, being able to discriminate a very large number of different states, will have a vast repertoire of possible states and the information brought by each will be extensive.

If Galileo and the photodiode are subjected to a very limited number of stimuli, the simple alternation between light and dark, the responses of the two systems may seem informative. To see the difference, therefore, it is necessary to establish as a condition that the repertoire of possible states of a system is calculated by disrupting the input peripheral devices of the system in all possible ways.

It must be emphasized that IIT is the antithesis of reductionism: even the fundamental unit of integrated information,  $\Phi$ , is a measure of irreducibility, which indicates if and how much the whole cannot be reduced to its parts.

One of the consequences of the theory is that consciousness is measurable in principle: the higher the value of integrated information  $\Phi$ , the higher the concept of consciousness. Theory can therefore be tested with facts. Thus a "consciousness meter", as primitive/simple/basic as it may be, has been developed which uses a transcranial magnetic stimulator and a large number of electrodes to read the integration of information from the brain responses.

In principle, IIT can serve to establish if and to what extent animals other than us are conscious, to clarify why consciousness has evolved and to explain why certain regions of the cerebral cortex are essential for consciousness and others are not.

Finally, the theory has important implications for artificial intelligence, which is hastily making new machines capable of equating and even exceeding our cognitive abilities.

The reason why a computer with a traditional Von Neumann architecture can never be conscious is in direct agreement with IIT, as its sequential structure prevents to reach a high integrated information value.

Consciousness is measured by considering how much actual information a set of elements can integrate, or how many states are available to a single integrated system, in terms of bits. Once one knows how to identify the integrated entities, one can go on to measure the complexity, that is, to see how much integrated information there is inside. At the end of the process you get a number associated with a particular set of elements.

The hypothesis is that complexity is distributed on a *continuum*, which is at a minimum in sleep without dreams and its maximum when wide awake.

### 1.3 THESIS OBJECTIVE

The measurement of  $\Phi$  has so far been carried out with computer simulation.

In this thesis, a first experimental method of measurement of IIT is proposed [18]. This objective is achieved by developing a coding method of states of consciousness that makes use of an Artificial Neural Network (ANN) to identify perceptive and cognitive events within EEG signals. The events are marked by chaotic attractors present in the

signals.

The ANN encodes them by assigning them with a binary code, attributing similar codes to similar events and distinct codes to distinct events.

Finally, the attractors identified in this way make it possible to calculate the quantity of  $\Phi$  for each event.



## 2 BRAIN AS DYNAMICAL SYSTEM

### 2.1 SELF-ORGANIZATION, COMPLEX SYSTEMS AND CHAOS

The theory of complex systems aims at analyzing and forecasting their behavior of the interaction among many elementary components, using mathematical and other formal tools. It also studies self-organization [19], i.e. the organization that emerges spontaneously from complex systems that, in the presence of suitable conditions, react to external environment changes reorganizing themselves [20] so as to exhibit novel properties [21].

A classic example is a fluid heated from the bottom. In the presence of appropriate boundary conditions, the convective motions of the molecules are arranged according to the so-called Bénard columns, that are vertical honeycomb formations. This unexpected cooperation between molecules is established whereas the system would simply be expected to increase in molecular disorder. The system reacted to the external environment modifications by reorganizing in such a way as to exhibit an innovative property.

Self-organization can be defined as a space-time structure that is not imposed from the outside but emerges spontaneously from the evolution of the system as a function of its dynamics [22]. The emerging organization is observable at a different space-time scale, much greater than the molecular one.

The development of mathematical models for such systems [23] shows that the equations that hold them are generally extremely sensitive to the initial conditions, so that extremely small fluctuations give rise to completely different dynamical stories (the famous Lorentz's "butterfly effect" [24]). This indeterminacy in real terms (but not in principle) is not avoidable, since for any numerical system a not infinite degree of precision must be fixed, and any degree, even the highest possible, will produce different dynamical stories. This represents the so-called "deterministic chaos": the system has a behavior altogether regular but irregular in detail, thus it is impossible to predict its future behavior.

We define *chaos* the unpredictable behavior of deterministic dynamical systems because of their sensitivity to initial conditions [25].

The behavior of a deterministic dynamical system is predictable once the initial conditions are known. But there are cases in which, depending on the precision in measuring the initial conditions, the motion of the system behaves very differently. More precisely, a set  $S$  exhibits sensitivity to the initial values if there is a neighborhood  $\rho$  such as for each  $\varepsilon > 0$  and for every  $x$  in  $S$ , there exists a  $y$  such that

$$|x - y| < \varepsilon \quad \text{and} \quad |x_n - y_n| > \rho \quad \text{for some } n > 0.$$

Then there is a fixed distance  $\rho$  such that, no matter how precisely an initial state is specified, there are neighboring states that eventually move away more than the distance  $\rho$ . This is what happens in chaotic systems.

A typical example of self-organization is present in all biological systems [26] and in their more evolved expression, intelligent life.

In addition, computational models are becoming more and more advanced, being able to simulate quite complex real systems.

A promising attempt to reproduce advanced functionalities by means of the collective behavior of simple elements is given, as specified below, by the Artificial Neural Networks paradigm: multiple interconnected elements exchange information on the basis of a series of input from the outside, and realize a form of functional organization that is not directly derivable from the algorithm imposed from the outside, but emerges from the complexity of the system.

## 2.2 COMPLEXITY AND NON-LINEARITY

In the traditional approach the complex systems are processed analytically, i.e. are reduced to a linear combination of elements. A classic linear relationship is the Hook's law ( $F = -kx$ , where  $x$  is the spring length and  $F$  the applied force) which regulates the elastic force. But when the elasticity is lost (e.g. straining the spring or the rubber band too much) the graph ceases to be linear. The system is not linear anymore, and in specific conditions it shows a sudden change of behavior: the rubber band breaks.

In nature many systems are linear or approximated to linearity (e.g. the electromagnetic wave equations), and this allowed the modeling of many natural phenomena. But for many physical systems linearity is not sustainable, and their modeling becomes extremely complex: as we will see in the following, almost all dynamical systems exhibit a chaotic behavior, i.e. they are not inherently nondeterministic, but in fact unpredictable [27] [28]. The processing of strongly time-varying and not strictly linear space-time patterns, such as those coming from the acquisition of real-world data, is an issue of growing importance, and its complexity involves necessarily the use and development of advanced mathematical tools.

The typical adaptivity of the Artificial Neural Networks and their generalization ability

seems to indicate them as a valid choice for the analysis of these systems. We will examine them in more detail in the following.

### 2.3 NON-LINEARITY AND DYNAMICAL SYSTEMS

We call linear the functions which behave in such a way that

$$f(ax + by) = af(x) + bf(y)$$

where this equality is not held, the function is called non-linear, and everything becomes mathematically more difficult.

For example if

$$f(x) = 0 \quad \text{and} \quad f(y) = 0$$

$f(ax + by)$  is no more equal to zero for any  $a$  and  $b$  (superposition principle: more solutions exist for each variable) and the solution must be sought with special methods.

A function that models real world is hardly linear, but is often approximated to a linear function. Non-linear systems exhibit complex effects that are not deducible with linear methods. This is particularly evident for dynamical systems [29] [30]. A system is called *dynamical system* when it expresses the variability of a state  $X$  (or a point in a vector space) in time:

$$\frac{dX}{dt} = F(x, t) \quad F : W \subset R^n \rightarrow R^n \quad \text{differentiable} \quad (1)$$

The solution of the system is the set of trajectories as a function of the initial conditions.

A dynamic system is completely defined by a *phase space* or *state space*, whose

coordinates describe it at all times, and by a rule that specifies the future trend of all the state variables.

Dynamic systems are said deterministic if there is only one solution for each state, stochastic if there are several solutions following a certain probability distribution (e.g. the toss of a coin).

The phase space is the collection of all possible states of a dynamic system. It can be finite (as in the case of the coin, two states) or infinite (if the variables are real numbers).

For example, a cellular automaton is a dynamic system with discrete time, discrete geometric space and discrete state space  $s(i, j)$ , where  $i$  are spatial coordinates,  $j$  is the time, and the update rule is

$$s(i, j + 1) = f(s) .$$

A simple example is the case of the pendulum, in which the phase space is continuous, two-dimensional and its coordinates are angle and speed.

If we include time as a coordinate of the phase space we represent the dynamic system with the above-mentioned differential equation (1), where  $(X, t)$  is the phase space.

Mathematically, a dynamic system is described by an initial value problem. The trajectory in the phase space traced by a solution of an initial value problem is called *trajectory* of the dynamic system.

We define constant trajectory a constant solution

$$x(t) = x(0)$$

of (1), i.e. a vector  $x(0)$  for which each component of the right side of (1) is zero.

A constant trajectory is said *stable* if the following conditions are met:

- a) there must be a positive number  $\varepsilon$  such that each trajectory beginning within  $\varepsilon$  of  $x(0)$  must asymptotically approach  $x(0)$ .
- b) for each positive number  $\varepsilon$  a positive number  $\delta(\varepsilon)$  must exist such that a trajectory is guaranteed to stay within  $\varepsilon$  of  $x(0)$  simply requiring it to start within  $\delta(\varepsilon)$  of  $x(0)$ .
- c) the set of all points that can be initial states of trajectories that asymptotically approach a stable trajectory is said *region of attraction* of the stable trajectory.

A *limit cycle*, or *cyclic attractor*, is a closed curve in the n-dimensional space with the following properties:

- a) no constant trajectory is contained in the limit cycle
- b) any trajectory that begins in a point of the limit cycle must lie within the limit cycle also later on
- c) for each positive number  $\varepsilon$  there must be a positive number  $\delta(\varepsilon)$  such that a trajectory is guaranteed to stay within  $\varepsilon$  of the limit cycle simply requiring it to begin within  $\delta(\varepsilon)$  of the limit cycle.

In summary, if some trajectories converge in some point, the set of initial states of these generated trajectories is said *region of attraction* of the point. A region of attraction is ultimately a set of points in the state space delimiting a finite diameter region such that each trajectory enters and never gets out.

### 2.3.1 Non-Linear Analytical Methods

A very common type of self-organization, which in nature is established also outside the life phenomena (e.g. involving meteorological and astronomical phenomena, fluid

dynamics, etc.), as mentioned above, is the deterministic chaos. The long-term behavior of the chaotic systems follows structured patterns detectable by displaying the system trajectories in the state space. These trajectories exhibit a spatial structure in which they are confined in a strange attractor (i.e. they exhibit some regularity but never repeat themselves exactly) [31]. A strange attractor is geometrically a fractal i.e. a structure with a non-integer dimension.

### 2.3.2 Fractal Dimension and Correlation Dimension

Define dimension  $D$  of an object the exponent which connects its extent  $b$  with the linear distance  $r$  :

$$b \propto r^D$$

The extent  $b$  can refer to the linear distance, area, volume, or the amount of information in bits. For a line  $b \propto r^1$  (and in fact a line has dimension 1), for a plan  $b \propto r^2$ , etc. Taking the logarithms we obtain.

$$D = \lim_{r \rightarrow 0} \frac{\log b}{\log r}$$

It is possible to have non-integer dimension objects, the so-called *fractals* [32], [33]. Their important feature is to be self-similar, i.e. they do not possess a characteristic scale. For example, a branch is a fractal object whose dimension ranges between 1 and 2. It is shown that chaotic attractors have a fractal (or Hausdorff) dimension  $> 2$ .

It has been shown for example that the fractal dimension of eyes-closed EEG (about 2) is lower than the open-eyes EEG dimension [34]. As we will see in detail below, according to W. Freeman [35], [36], [37] a chaotic brain activity prepares for the perception of a particular stimulus, and its trajectories end up within a periodic (limit cycle) or chaotic basin of attraction. Even time series may exhibit characteristics of stochasticity or chaotic organization [38].

To assess the dimension of a series, a procedure called *delay-time embedding* is used. If a time series is long enough, the trajectory of the state space generated by it is geometrically equivalent to the attractor of the system that generated the original series.

Grassberger and Procaccia [39] have developed a method, often applied to physiological data, which allows to determine the so-called *D2 correlation dimension* (which corresponds to a lower limit for the fractal dimension).

We replace each observation in the original signal  $X(t)$  with the vector:

$$y(i) = x(i), x(i+d), x(i+2d), \dots, x(i+(m-1)d)$$

obtaining as a result a series of vectors of  $m$  coordinates in an  $m$ -dimensional space:

$$Y = y(1), y(2), \dots, y(N - (m-1)d)$$

$$n=2d+1.$$

where  $N$  is the length of the original series and  $d$  the so-called *lag* or *delay time*, i.e. the number of points between the components of each reconstructed state vector.



It can be shown that the reconstructed state vectors are topologically invariant transformations of the original state vectors, and that the set of state vectors (points in the  $m$ -dimensional space) formed by  $Y$  in the reconstructed space has the same dimension of the attractor of the system.

It also demonstrates (Taken's Theorem) that there is a mathematical relationship between the embedding dimension  $n$  of the series and the dimension of the attractor of the corresponding dynamic system:

Now, the dimension  $D2$  is defined as

$$D2 = \lim_{r \rightarrow 0} \frac{\log C(r)}{\log r}$$

where the extension of the series is given by the *correlation integral*  $C(r)$ .

The correlation integral is calculated as the average number of state vectors that stay within a distance  $r$  from each other. In other words,  $C(r)$  calculates the average number of points that are on the corresponding reconstructed attractor. If the attractor is a fractal, for a certain range of  $r$  (the range in which fractals are perfectly self-similar) the logarithm of this average will have a linear relationship with the logarithm of  $r$ .

In this region the slope of the curve measures the *correlation dimension*  $D2$ . The correlation dimension  $D2$  gives the measure of the complexity of the system attractor and, in the way shown above, is connected to the correlation integral, which instead measures the extension of the attractor.

The graph of the correlation dimension is expressed as a function of the embedding dimension. Ideally, the graph should converge asymptotically to the real correlation dimension.

In a time series the concept of self-similarity is used in a distributional sense: if viewed at a different scale, the object distribution remains unchanged.

In such a case a long-range dependency occurs, i.e. the values at each instant are correlated to the values of all the successive instants.

A self-similar time series has the property that when aggregated into a shorter series (where each point is the sum of multiple original points) it maintains the same autocorrelation function

$$r(k) = E[(X_t - \mu)(X_{t+k} - \mu)]$$

both in the series  $X = (X_t: t = 0, 1, 2, \dots)$  and in the contracted series  $X^{(m)} = (X_k^{(m)}: k = 1, 2, 3, \dots)$ , aggregated in blocks of size  $m$ . So, the series is distributionally self-similar, because the distribution of the aggregate series is the same (except for a scale variation) as the original.

As a result, the self-similar processes show long-range dependency, i.e. have an autocorrelation function,

$$r(k) \sim k^{-\beta} \text{ for } k \rightarrow \infty \quad 0 < \beta < 1$$

i.e. the function decays hyperbolically.

## 2.4 ARTIFICIAL NEURAL NETWORKS AS DYNAMICAL SYSTEMS

### 2.4.1 Stability and Regions of Attraction in Neural Models

An Artificial Neural Network (ANN) can be seen as a dynamic system which gives account for the dynamics of  $n$  neurons.

Each neuron is mathematically defined by its state  $x(i)$  and its function  $g = g(x_i)$  (gain) differentiable everywhere and non-decreasing. A typical gain function is the logistic function

$$g(x) = \left(1 + e^{-x}\right)^{-1}$$

This feature provides values between 0 and 1. But it is often useful to use a transfer function symmetrical with respect to zero, so to keep any symmetry of the input values. Thus, the hyperbolic tangent function (values between -1 and +1) is used, or the function

$$F(P) = \frac{A(e^{kp} - 1)}{(e^{kp} + 1)}$$

with positive constants  $A$  and  $k$ .

The rate of change of each  $x_i$  is determined by a function dependent on  $x_i$  and on the outputs  $g_i(x_i)$ . In general, we can express this change with the system of differential equations

$$\frac{dx_i}{dt} = -k_i x_i + p_i(g(x)) \quad (2)$$

where  $k_i$  is a positive constant, and each  $p_i$  is an in general polynomial function of  $n$  variables  $g_1(x(t), g_2(x(t), \dots, g_n(x(t)))$ , which behave well enough to make sure that the trajectories for the system of equations exist and are unique.

By trajectory, we mean a series of points in an  $n$ -dimensional space that depart from some initial state (at time zero) in the  $n$ -space to a final state. The task of the Artificial Neural Network is to generate such a set of points up to the final state, which constitutes the output of the network.

The levels of activity of  $n$  neurons are represented by a point in the  $n$ -dimensional space [40]. Therefore, we build an  $n$ -dimensional dynamic system which solutions are trajectories representing constant attractors (stable equilibrium) or cyclic attractors (limit cycles).

We say that *the purpose of the Artificial Neural Network is to generate trajectories in the  $n$ -dimensional space that are asymptotically approaching some of the constant attractor trajectories.*

In the additive neural models (as the Multilayer Perceptron, see below) each  $p_i$  is a linear function of the components of  $g$ :

$$p_i = \sum_j^n T_{ij} g_j \quad (3)$$

where  $T_{ij}$  are real constants forming an  $n \times n$  matrix.

However, recently higher order Artificial Neural Networks have emerged as more

efficient. In this kind of networks, each  $p_i$  is a polynomial function of the components of  $g$ : typically of the form

$$g_1^{e_1} g_2^{e_2} \dots g_n^{e_n}$$

where each exponent  $e_i$  is 0 or 1.

For linear networks of the type (3) the Cohen-Grossberg theorem [41] ensures the existence of stable points, i.e. points such that

$$\frac{dx(P)}{dt} = 0$$

#### 2.4.2 Cohen-Grossberg THEOREM

Every dynamical system of the form

$$\frac{dx_i}{dt} = a_i(x_i)[b_i(x_i) - \sum_j w_{ij} S_{ij}(x_j)]$$

s.t.

- 1) The matrix  $w_{ij}$  is symmetrical and each  $w_{ij} \geq 0$
- 2) The function  $a_j(x)$  is continuous for  $x \geq 0$  and  $a_j(x) > 0$  for  $x > 0$
- 3) The function  $b_j(x)$  is continuous and does not tend to infinity for any open interval for  $x > 0$
- 4) The function  $S_{ij}(x)$  is differentiable and  $S'_{ij}(x) > 0$  for  $x \geq 0$

5)  $b_i(x) - W_i S_i < 0$  for  $x \rightarrow \infty$  has an at least countable set of stable points  $P$  such that

$$\frac{dx(P)}{dt} = 0$$

If the network status at time 0 is such that  $x_i(0) > 0$ , then the ANN will converge usually at some stable point  $P$  (i.e. such that  $\frac{dx(P)}{dt} = 0$ ), and at least a countable set of such points will exist.

Although these conditions are restrictive, they match those supported by many hetero- and auto-associative ANNs (see below the Hopfield network, with fully interconnected nodes and symmetrical weights).

The memories are set in the attractors, and the theorem guarantees their existence, although there are many spurious attractors (Fig. 2-1).

To any state of a network an energy Lyapounov function can be associated that allows you to determine certain properties of the trajectories. A Lyapounov function  $L$  is a function:

$$L: \{0,1\}^n \rightarrow R \quad , \quad L(T(x)) \leq L(x)$$

for each  $x \in \{0,1\}^n$ , where  $T$  is the transition function operated by the network.

Thus,  $L$  is monotone non-increasing along each trajectory. It follows that the equilibrium points of the system correspond to the minimum points of  $L$ . For networks with a square connection matrix, the  $L$  function is called energy function and is chosen as

$$E(x) = -\frac{1}{2} \sum_i \sum_j w_{ij} x_i x_j$$

where one can easily see that it is monotone non-increasing and  $\Delta E \leq 0$  anytime, i.e. the system is globally stable.

This is the case for the Hopfield network [31], an obvious example of how an ANN is a dynamic system that can tend to a series of stable attractors.

It is a fully connected network with symmetrical weights, with bipolar input (+/- 1 or 0/1).

The inputs are simultaneously applied to all nodes, and the weights are set according to the law

$$w_{ij} = \sum x_i x_j \quad \text{for } i \neq j$$

$$w_{ij} = 0 \quad \text{for } i = j$$

In the learning cycle each output of a neuron is a new input for the same neuron. The calculation of the new value is established by the function

$$f(x_i) = x_i \quad \text{if} \quad \sum w_{ij} x_j = T_i$$

(threshold possibly equal to zero)

$$f(x_i) = +1 \quad \text{if} \quad \sum w_{ij} x_j > T_i$$

$$f(x_i) = -1 \quad \text{if} \quad \sum w_{ij} x_j < T_i$$

We can see an input pattern as a point in the state space that, while the network iterates, moves gradually toward minima, which represent stable states of the network. The last values of the weights represent the output of the network. The solution occurs when the point moves to the lowest region of the basin of attraction.

In fact, as for symmetric matrices with diagonal equal to zero

$$\frac{\Delta E}{\Delta x_i} = -\sum w_{ij}x_j$$

if  $\Delta x_i < 0$  then  $\sum w_{ij}x_j < 0$   
 if  $\Delta x_i > 0$  then  $\sum w_{ij}x_j > 0$

i.e. always  $\Delta E \leq 0$ .

After a number of iterations the network will stabilize in a state of minimum energy. Each minimum corresponds to a pattern stored in the network. An unknown pattern constitutes a point on this hyperplane, which gradually moves toward a minimum. There may be so-called metastable states, i.e. minimum points that don't have a corresponding stored pattern (spurious attractors).

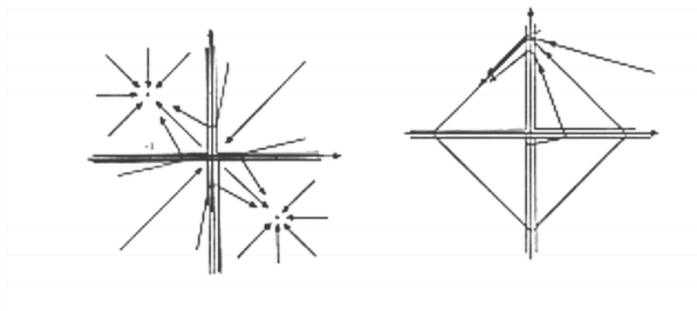


Figure 2-1 Typical trajectories in a two dimensional space with two memories and a limit cycle model

More generally the following theorem holds:

**THEOREM:**

Each ANN model of type (2) has a finite region of attraction.



## *Learning*

Once a particular dynamic model and its attractors have been identified, a learning algorithm is to be established that varies the locations of fixed points to encode information. Therefore, a condition sufficient for the existence of such an algorithm is the existence of isolated stable attractors in the system, i.e. of fixed points.

The weight matrix is to be adjusted in such a way as, given an initial state  $x_0=x(t_0)$ , a fixed point  $x_\infty=x(t_\infty)$  corresponds to a given input, and the fixed point has components that have a desired set of values  $D_i$  in the output units.

A typical method, used in the backpropagation networks [30], is to minimize a function  $E$  that measures the distance between the desired fixed point (attractor) and the current fixed point:

$$E = \frac{1}{2} \sum_i J_i^2$$

where

$$J_i = (D_i - x_{i\infty}) Q_i$$

and  $Q_i$  is a function which value is 1 or 0 according to whether the  $i$ -th unit belongs or not to the output subset of the network units.

Then the learning algorithm will move the fixed points so as to satisfy on the output units the equation

$$x(t_\infty) = D_i \ .$$

A typical way to do this is to let the system evolve in the weight space along the

trajectories antiparallel to the gradient of  $E$ :

$$\tau \frac{dw_{ij}}{dt} = - \frac{dE}{dw_{ij}}$$

where  $\tau$  is a numeric constant that defines the temporal scale with which the weights are changing.  $\tau$  must be small, so that  $x$  could always be substantially constant, i.e.

$$x(t_{\infty}) = x_{\infty}.$$

When on the output layer the error is computed between current output and desired output, this is propagated backwards to the other layers, in such a way as to adjust weights of any single node.

This algorithm, that is called gradient descent, is used by the backpropagation networks; it is not the only possible algorithm but is no doubt the easiest and most effective equation for the minimization of  $E$  [42] [43].

It can be shown that, if the initial network is stable, the gradient descent dynamics does not change the network stability.

This allows to state the reliability of the backpropagation algorithm, that yields the necessary robustness to the deviations generated by the noise present in real data.

### 2.4.3 Neural Models of Dynamical Systems Processing: Spatiotemporal

#### Patterns in Artificial Neural Networks.

ANNs have been initially applied to problems regarding spatial or instantaneous patterns, but the evolution of technology has made it necessary to apply them also to

spatiotemporal pattern. By spatiotemporal pattern we mean a function  $x(t)$  that associates at any time  $t$  a point in the  $n$ -dimensional input space:

$$x(t):\{t_0, t_1\} \rightarrow R^n$$

In three dimensions, it is possible to represent a spatiotemporal pattern as a trajectory in the input space parameterized as a function of time. The task of the ANN will be to implement a time-variant transformation, that associates an output function  $y(t)$  to the function  $x(t)$  for each time  $t$ .

Several methods have been proposed in the past to allow the ANNs to process the spatiotemporal patterns, i.e. to generate parameterized attractor trajectories over time.

These methods can be classified mainly in the following variants [44]:

- Creation of a spatial representation of temporal data
- Setting of time-delays in neurons or connections
- Use of neurons with activations that add up the inputs over time
- Combinations of the above methods.

The earliest strategy was to convert the output data into a sequence of data. When a new set of inputs is received, the previous data are deleted and so on. The network preserves the memory of the past only in the intermediate layers.

Then the so-called time-delay networks were studied, in which the information at an instant of time is moved to the right in a chain of nodes, while the new information is added to the left. The number of nodes determines the number of time intervals on which information is sampled.

An architecture that leads to stable states without time-delay can produce oscillations or a chaotic behavior (with cyclic or chaotic attractors) once the delay is introduced. Instead, if

the delay is transmitted in the connections, the information remains in a certain state for a period, then a connection is triggered that brings it to another state and so on. It can be proved that such networks, which are obviously equipped with long or short-term memory, are able to reproduce different types of temporal sequences.

Another method is to change the neurons in such a way that they are able to add up data that arrive through time, allowing a gradual decay of the older information.

If neurons have recurrent connections, the feedback acts creating hysteresis in each neuron, thus a memory of the information that persists beyond the stimulus.

ANNs have also been proposed that accept input information coded in the form of frequencies, as actually occurs in the natural sensors.

These networks were used to drive robotic actuators, with good results in the hardware implementation. The simplest of the above described ANNs are networks not equipped with memory, with static architecture, which does not include any actual management of the time variable [44].

#### 2.4.4 Neural Models of Dynamical Systems Processing: Recurrent Neural Networks

The so-called dynamical (in the strict sense) networks have proved to be more efficient in processing time-dependent inputs. Their architecture [45] is characterized by a feedback system called state feedback (Fig. 2-2), achieved through appropriate connections between the nodes. It consists of the fact that a node receives as afferent signals both the inputs and all the outputs of the other nodes, including its own. An internal state of the network becomes definable, which all the nodes in the network with their current outputs

contribute to. These networks can be described by differential equations of the type where  $u_i(t)$  is the internal state of the  $i$ -th unit,  $t_i$  is the time constant of the  $i$ -th unit,  $w_{ij}$  are the connection weights,  $I_i(t)$  is the input of the  $i$ -th unit and  $g(u_j(t))$  is the output of the  $i$ -th unit.

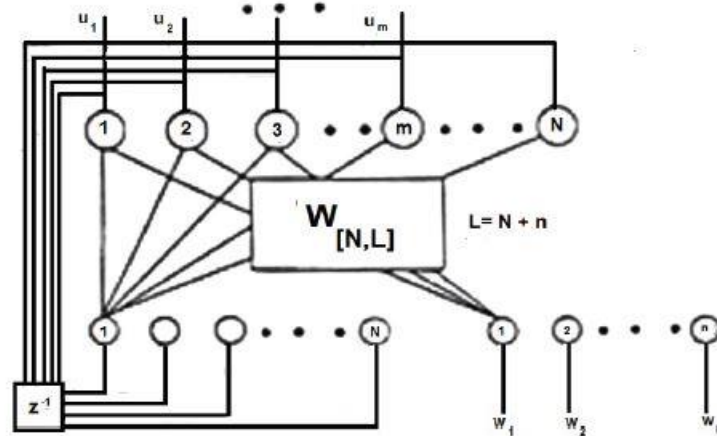


Figure 2-2 Recurrent network with state feedback

Pineda [46] shows that this system of equations is reduced to the system (2) through a simple linear transformation.

Recurrent neural networks are ultimately nothing more than networks that possess complex connections between the nodes, in contrast to the feedforward networks which bind the connections to a single direction (from input towards the output) [47].

This model includes a large class of ANNs.

As mentioned, Recurrent neural networks give better performances than feedforward networks in the treatment of spatiotemporal pattern and in general in the modeling of real dynamic systems. For such systems theorems exist ([48] [49]) showing that time-finite trajectories of a given  $n$ -dimensional dynamical system are approximated by the internal states of the output units of a Recurrent network with  $n$  units of output,  $N$  hidden nodes

and appropriate initial states.

In this way the theorem of existence of attractors in the case of Recurrent neural networks is guaranteed by the same theorem (4).

The multilayer perceptron (MLP) is suitable to be turned into a Recurrent neural network according to various possible schemes, the more classic of which is due to K. Narendra [50] and is visible in Fig. 2-3:

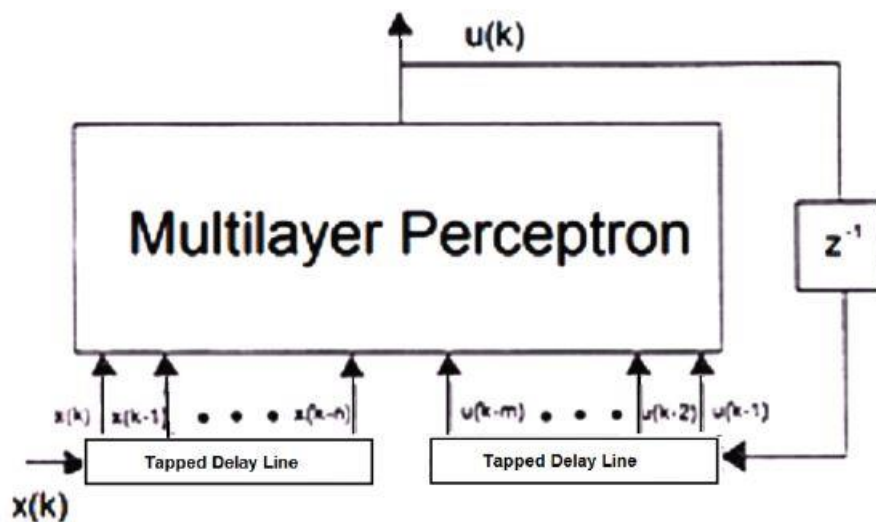


Figure 2-3 Narendra Architecture

The input layer is connected to a tapped delay line, where the sequence of data to be processed is flowing. In another delay line flow the output observations. The only output  $u(k)$  is function of the  $n$  input observations and of the  $m$  previous outputs. The  $n+m$ -ple of inputs is interpretable as a point in the input space.

Following the method introduced by Williams and improved by Pineda [51], [52], [46] the following model is obtained.

The node equation is

$$u(k+1) = f(\sum w_{ij}u_j(k) + v_i(k)) \quad 0 \leq k \leq n$$

The first layer output is

$$z_j = u_j(k) \quad 0 \leq j \leq N$$

$$z_j = v_j(k) \quad N+1 \leq j \leq L$$

where  $z_j$  is the output of the first layer and  $v_j$  the current input.

The current output is

$$u'_i(k+1) = f(I_i(k))$$

where

$$I_i(k) = \sum_j w_{ij} z_j(k) + z_0 \quad (z_0 \text{ bias})$$

and the node equation is

$$u_i(k+1) = f(I_i(k))$$

where  $f$  is sigmoid function. The learning algorithm is similar to that of the static MLP.

Despite Recurrent networks are an advanced treatment method for spatiotemporal patterns [47], high variability in the data limits the performance of this ANN model in

the use in real time due to the difficulty of finding an exhaustive training set and/or to the

length of the learning process [53].

Applications suffer from severe limitations in computational speed or alternately in the ability to adapt to input fluctuations, being difficult to arrive at a positive compromise between the slow online learning process and the poor off-line learning performances. This issue is intrinsic to the supervised learning method.

#### 2.4.5 Self-Organizing Networks

An almost forced alternative to the limits of this architecture seems to be constituted by the unsupervised ANNs [54] [55], whose most classical and still effective explication remains currently the Self-Organizing Map (SOM) of T. Kohonen.

The SOM was developed in the 80s by T. Kohonen [56] based on previous studies of neurophysiology. In fact the SOM mechanism was written taking into account the neurophysiological mapping of sensory stimuli on the neocortex, where similar inputs are mapped to nearby locations of the cortex in an orderly and topology-conservative fashion. The structure of a Kohonen network consists of a layer of  $N$  elements, said competitive layer. Each of these receives  $n$  signals  $x_1, \dots, x_n$  that originate from an input layer of  $n$  elements, whose connections have weight  $w_{ij}$  (Fig. 2-4).

If the competitive layer has a matrix topology, neurons are connected to each other in a square, hexagonal or rhomboid pattern. If they are vector-based, neurons are simply connected together to form a chain.

To estimate the input intensity  $I_i$  of each of the Kohonen layer elements the process is as follows:



$$I_i = D(w_i, x)$$

$$w_i = (w_{i_1}, \dots, w_{i_n})^T$$

$$x_i = (x_1, \dots, x_n)^T$$

where  $D(u, x)$  is some distance function, e.g. the Euclidean one.

At this point a competition is put in place to assess which element has the smaller intensity input (i.e. which  $w_i$  is the nearest to  $x$ ).

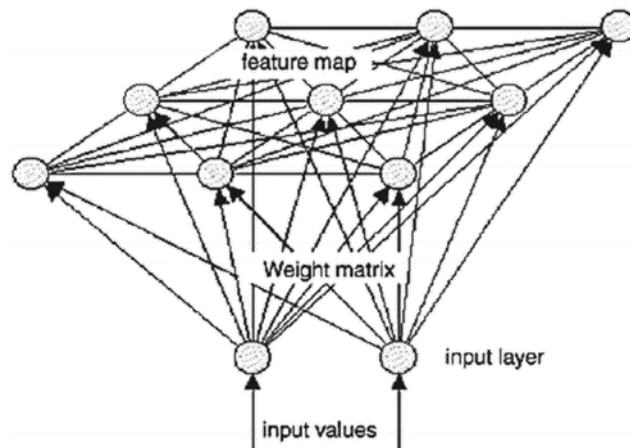


Figure 2-4 Kohonen Self organizing Map

In this architecture, each element receives excitatory stimuli from the adjacent elements (the so-called neighborhood).

The existence of the neighborhood is useful not to polarize the network on a few winning neurons.

In this way only the elements with distance below a certain value are activated, or in restrictive cases only the unit with minimum distance is activated. At this point the learning phase takes place, according to the so-called "Winner Take All" law (WTA).

The training data consist of a sequence of input vectors  $x$ . The Kohonen layer then decides the winner neuron on the basis of the minimum distance. Now the weights are modified according to the law

$$w_{i_{new}} = w_{i_{old}} + \alpha(x - w_{i_{old}})z_i$$

where  $0 < \alpha < 1$  slowly decreases over time with the law

$$\alpha(t) = \alpha[1 - t/\delta]$$

where  $\delta$  is a suitable constant. Being  $z_i \neq 0$  only for the winning neuron, the weights of the winning neurons rotate more and more towards the closest vectors, up to ideally overlap with them (Fig. 2-5).

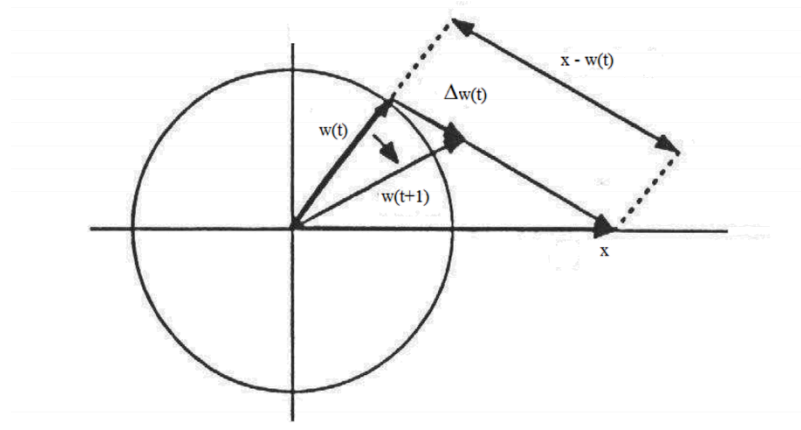


Figure 2-5 Rotation of the weight vectors

In this way the SOM performs a vector quantization, that is a mapping from a space with many dimensions to a space with a smaller number of dimensions, preserving the initial

topology.

In other words a Nearest Neighbor (NN) form of clustering is carried out, in which each element of the competitive layer represents the class of the input elements.

The NN method classifies a pattern according to the smallest value obtained among all the distances from a set of reference patterns. This method is useful for separating classes representable by segments of hyperplanes.

For this reason, the SOM classifies correctly pattern topologically well distributed, but shows difficulties in the case of non-linear distributions.

Moreover the importance of the initial weight configuration appears evident, as it must be the most similar to the input topology.

#### 2.4.6 The ITSOM Architecture

Various are, however, the reasons which in turn limit the SOM performances in the case of strictly non-linear and time-varying input. The first reason is that if the non-linearity of the input topology is too accentuated, the competitive layer is not capable to disentangle itself enough on the form of that topology.

The second reason concerns the difficulty of ensuring convergence (due to the lack of ability to establish a network error for each epoch). The third reason is the low output cardinality, limited to number of competitive layer neurons.

Another problem of the SOM, typical of any clustering algorithm, and the lack of output explication. Once the classification output is obtained, the user must extrapolate the significance with an ad-hoc procedure, which in real-time applications can further penalize the computational load.

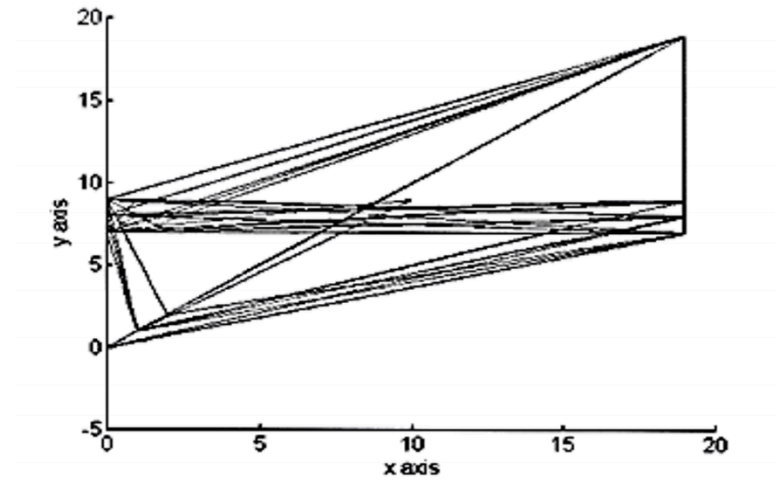


Figure 2-6 Series of the winning neurons in 2-dimensional state space - x axis and y axis  
 indicate the weight order  $e$  values

A proven successful solution was found observing the time series the SOM winning neurons epoch after epoch (Fig. 2-6). It can be shown in fact that this series forms attractors that hold through epochs and that identify univocally the input pattern that generated them. On the basis of this evidence the ITSOM (Inductive Tracing Self-Organizing Map) model was developed, whose architecture is described below.

The time sequence of the SOM winning neurons tends to repeat creating chaotic attractors or precise limit cycles that uniquely characterize the input that produced them: in fact, the learning rule implies that the winning weight represents an approximation of the input.

At every epoch the new winning weight, along with the weight that won in the previous epoch, constitutes a second order approximation of the input value, and so on.

So it is possible to derive the input value by comparing the characteristic configurations of each input with a set of reference configurations, whose value is known.

In this way a real process of induction is realized, because once a vector quantization many-to-few from the input layer on the weight layer is carried out, a few-to-many step is

operated from reference configurations to the whole input (Fig. 2-7).

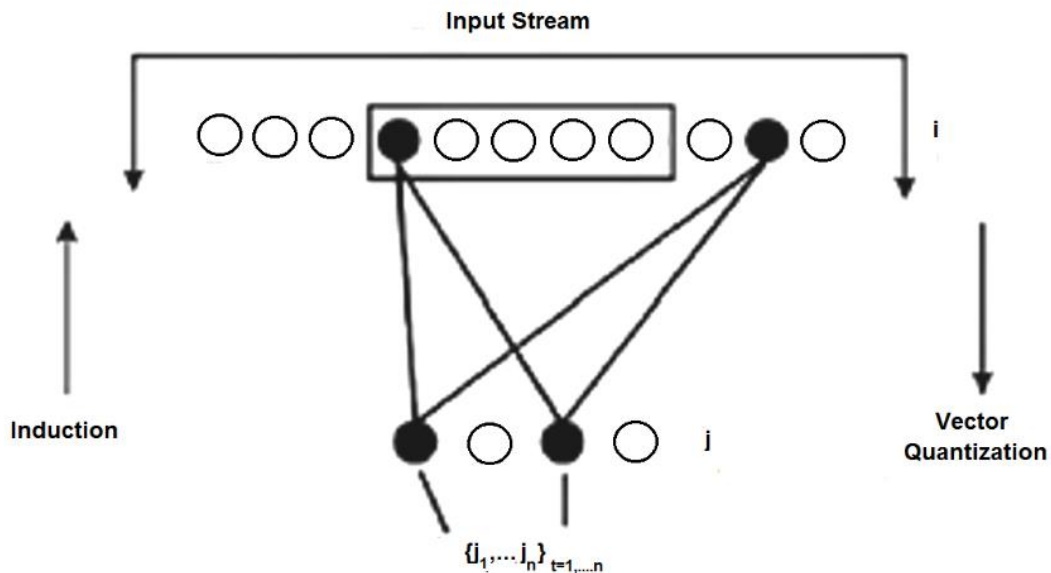


Figure 2-7 ITSOM Architecture

This form of induction is much finer than that obtainable from the only final winning neurons of the a SOM network, because the choice among a set of competitive layer neurons is too limited to provide a meaningful classification.

Instead the possible ITSOM outputs are  $2^n$  where  $n$  is the number of neurons of the competitive layer, that make it possible to finely discriminate the input features.

It should be emphasized that the ITSOM does not need to be brought to convergence, because the winning neurons configurations reach the necessary stability within a few tens of epochs.

It was verified that for best results the network should not polarize on too few neurons but even not disperse throughout the layer.

The best suited algorithm to recognize the configurations created by the network is based

on the z-score method.

The cumulative scores for each input are normalized according to the distribution of the standardized variable  $z$  given by

$$z = \frac{(x - \mu)}{\sigma}$$

where  $x$  is the input,  $\mu$  is the average of the scores on the neurons of the competitive layer and  $\sigma$  is the standard deviation.

Once set a threshold  $0 < \tau \leq 1$ , which therefore constitutes one of the parameters of this type of network, we put

$$\begin{aligned} z &= 1 \quad \text{for } z > \tau \\ z &= 0 \quad \text{for } z \leq \tau \end{aligned}$$

In this way, each configuration of winning neurons is represented by a binary number formed by as many ones and zeros as many the output layer neurons.

Then it is immediate to use these binary numbers as templates of the input patterns.

Both SOM and other ANNs base their learning process on the cyclic repetition of the input stimulus. Even in the brain there is evidence of reverberating circuits that strengthen the input information on the cortical map.

However it seems unlikely that these loops can be repeated thousands of times in search of a fixed target, also because it is difficult to support the hypothesis that the brain recognizes the last activated neuron as the only information carrier.

It appears more reasonable that the reverberation activities run out spontaneously with the

exhaustion of the electrical firing process, and that the cortical maps is formed by a constellation of activated neurons, the so-called mnestic traces, which in the following will be used to recover information.

For this reason the ITSOM mechanism may appear more physiologically justified.

On the other hand the fact that learning can be both supervised and unsupervised seems confirmed by the everyday experience and by several studies [57] [58] [59] [60] [61] [62].

But ITSOM can also be used in a supervised fashion, as it can learn from a set of examples and the obtained z-scores can be used to recognized new patterns [63] [64].

#### 2.4.7 Dynamical Analysis of ITSOM

The SOM can be expressed as a non-linear dynamic model expressed by the differential equation [65] [66].

$$\frac{dx_i}{dt} = I_i - \mu(x_i)$$

where the output variable  $x_i$  can be matched to the average firing rate of the neuron  $i$ ,  $I_i$  is the combined effect of all inputs to the neuron  $i$ , and  $\mu(x_i)$  the sum of all the non-linear losses of the firing process.

As mentioned above, the SOM architecture was studied by T. Kohonen following his neurophysiological studies, observing the WTA function in the cortex [67].

B. Ermentrout [68] studied a cortical model in which the WTA process has the dual role

of selecting the most important stimulus and strengthening the patterns after the disappearance of the stimulus.

The author shows that every time a neuron is active for a certain time and then stops firing, the network oscillates between different states, as "ponies on a merry-go-round".

The author explains that the limit cycles that are created are the effect of the bifurcation solutions of system.

$$\frac{dx_i}{dt} = -\mu x_j + F(x_j, u(t); \alpha) \quad j = 1, \dots, N$$

for  $N$  activated neurons  $x_j$ , where  $F(x, y; \alpha)$  is a function of two variables parameterized by  $\alpha$  and such that

$$\frac{F(\cdot)}{dx} > 0 \quad \text{and} \quad \frac{F(\cdot)}{dy} < 0,$$

and  $u(t)$  is the inhibitory feedback of the form

$$u(t) = G\left(\sum_k x_k\right)$$

where  $G$  is monotonically increasing.

The overall activity  $x_1(t) + \dots + x_j(t)$  is shown to lie almost on a closed trajectory, that means that the total excitatory network activity remains almost constant.



#### 2.4.8 Non-Linear Analysis of Cortical Signals and Functional Binding of Perceptions

An application of the non-linear analysis methods has been tested in the study of the so-called binding problem, i.e. the problem of understanding the origin of the perceptual unity of consciousness in the multiplicity of sensory stimuli.

Many neurophysiologists [69] [70] [71] [70] [72] [73] [74] [75] have proposed that such unity can be related to the self-organization of gamma waves (~ 40 Hz) emitted by the cortical neurons, which in many studies show to synchronize under sensory stimuli among distant sites, and may therefore create a functional binding.

It was proposed that the oscillation activity at high frequency in the cortex may be linked to the functional binding related to high-level cognitive functions such as memory and learning.

Global coherent patterns of neuronal activity are considered by influent neuroscientists as the main neural correlate of conscious experience [36], [37].

The ability to simultaneously record the activity of distant cortex sites through microelectrodes led to the possibility to analyze the mechanism by which the activity of a collection of neurons can be coordinated in a unique pattern.

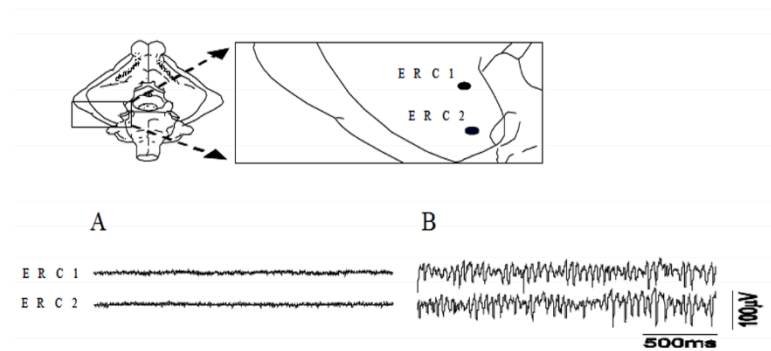
It was proposed that neurons in the sensory cortex interact extensively and that the action potentials evoked by stimuli lead to the emergence of a self-organized pattern of activity as a cortical response to the stimulus [69].

In order to evaluate the possible correlations in the neural signals the above described ITSON network model was used, to highlight the presence of limit cycles or chaotic attractors [76].

Electrophysiological signals were obtained from the brains of guinea pig isolated

artificially [70]. It was seen that the gamma activity can be induced in the median entorhinal cortex (ERC) of guinea pigs which is administered carbachol (50-100 mM), simulating the attentional activity in the presence of a sensory stimulus.

The gamma activity is recorded simultaneously at different points (up to 20) separated by about 1mm in the median ERC [71] (Fig. 2-8)..



*Figure 2-8 Entorhinal median cortex signals before and after carbachol administration*

Several files derived from 4 different monitoring sites in the entorhinal cortex were recorded before, during and after the administration of carbachol, simulation of an attentional stimulation.

The signals were considered simultaneously on all recording sites to assess their correlation.

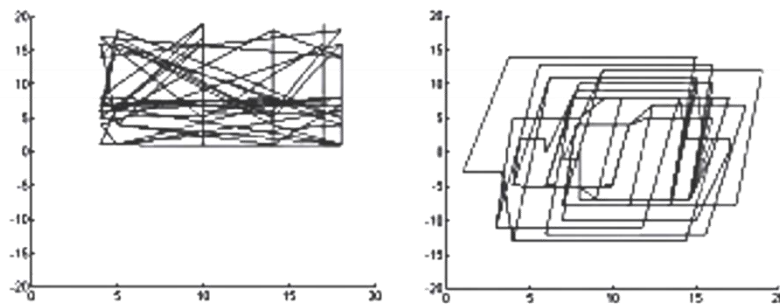
The same records were used as input for the ITSOM network, and the time series of the winning neurons was processed with a MATLAB/SIMULINK procedure.

The procedure allowed to highlight the presence of limit cycles or chaotic attractors, displaying their trajectory in the phase space.

Under control conditions (before the activation of the fast oscillations), the graphs show

some organization on the single record, but patterns with random structure or poorly organized appear in case of signals processed simultaneously from multiple sites.

However, after the induction of oscillatory activity through the application of carbachol, more chaotic patterns appear, with similar but never identical values, and strongly symmetrical shapes (Fig. 2-9).



*Figure 2-9 State space attractors before and after carbachol administration*

In order to quantitatively evaluate the attractors, Hurst parameter, correlation dimension and Recurrence Quantitative Analysis [77] have been used.

The Hurst parameter, constantly under the value of 0.4 before carbachol, grows sharply after carbachol and exceeded the threshold of 0.5, often reaching 0.8. This indicates that the signals become organized during the stimulus and keep the organization for a time after the stimulus.

The correlation dimension does not appear to be a significant parameter because it keeps constant in the range 2.6-3.2 (using 10 as the embedding dimension value) before and after the stimulus: this value seems to be a feature of the type of signal.

It should be noted that the  $size > 2$  shows a generic chaotic behavior of the series.

On the other hand the measurement of determinism of the embedded series, evaluated with the Recurrent Quantification Analysis, confirms the same increase after the stimulus

shown by the Hurst parameter, jumping up to over 90% and keeping this very high value for a time.

The analysis of the original time series with linear methods tested on distant sites confirms an increase in values after the stimulus but is maintained lower than 0.4 in all tests. The non-linear analysis on the single record or two records carried out with the calculus of correlation dimension, Hurst parameter and Recurrence Quantification Analysis essentially confirms the ITSOM results.

In some cases sharp differences of the parameter values have been detected whose neurophysiological meaning is not known and should be investigated more closely.

In general, we can conclude that the ITSOM network identifies self-organizing structures more often than linear numerical analysis. This may suggest a finer sensitivity of ANNs, although the possibility of false positives cannot be ruled out.

On the other hand, the values of the Hurst parameter derived from the ITSOM are often higher than the corresponding values derived from the original series.

It should also be pointed out that, unlike non-linear analysis on the original series, the analysis carried out with the ANN made it possible to simultaneously analyze all the recording sites, testing their possible synchronicity.

It is also possible, once an organized pattern is found, to identify it by its z-score and to recognize the same attractor every time the set of signals generates one.

In conclusion, the existence of a non-linear coherence (in the form of chaotic attractors) in rapid oscillations induced on guinea pig cortex is confirmed, suggesting a possible functional binding of chaotic nature between distant regions of the entorhinal cortex. The ITSOM method can test the coherence of records simultaneously from all sites. It is also possible to deepen the analysis of the meaning of these patterns through the possibility to compare similar attractors in time.

W. Freeman researches ( [35] and subsequent work) have proposed, through a study with microelectrodes implanted on the cortex of rabbits and recorded during the experimental release of smells, that cortical neurons interact extensively highlighting chaotic spatiotemporal patterns, repetitive in correspondence of a specific smell and different in response to different stimuli.

The ITSOM ANN non-linear analysis confirms the hypothesis that the coordinated 40 Hz activity of cortical neurons may clarify the origin of the sensory "binding" that we all perceive. It is also possible to deepen the analysis of the meaning of these patterns through the possibility to compare similar attractors in time.

### 3 THE EXPERIMENTAL PHASE

The goal of this work is to process signals in order to detect and quantify their information (and in some way their consciousness) content. For this purpose we carried out an experimental phase devoted to obtain recorded digital EEG signals from human subjects.

#### 3.1 EMOTIV EPOC +

The instrument that has been used for recording EEG signals is EMOTIV EPOC +. The signals amplitudes are recorded during the administration of two videos: the first consists of primary colors with different shades, the second experiment with colors and images of emotional and sensorial appeal.

In this project we processed signals from 14 electrodes of the wireless EEG system [78] (Fig. 3-1). The EMOTIV EPOC + offers a headset with 14 electrodes plus a reference, a single set of electrode felts, and a USB receiver for recording data on a PC has a frequency of sampling equal to 2048 Hz with a resolution of 14 Bits, with a notch set between the 50 and the 60 Hz. The electrodes provided are at international 10-20 locations: AF3, F7, F3, FC5, T7, P7, O1, O2, P8, T8, FC6, F4, F8, AF4. There is a fixed reference electrode at P3 (Emotiv labels for the CMS or “common mode sense”) and a

“driven right leg” (DRL) at P4. The CMS is the actual electrical reference for the EEG recordings, the DRL provides a feedback noise cancellation system and is not a reference in the EEG sense. The EMOTIV EPOC + uses saline felt electrodes. The electrodes are gold-plated disks, and a round felt, wetted with saline, is placed in between this disk and the scalp.



*Figure 3-1 The EMOTIV EPOC +*

The EEG signals received from the headset are transferred to a computer through a wireless USB dongle. These properties along with it being lightweight make the EPOC extremely portable and easy to use [78].

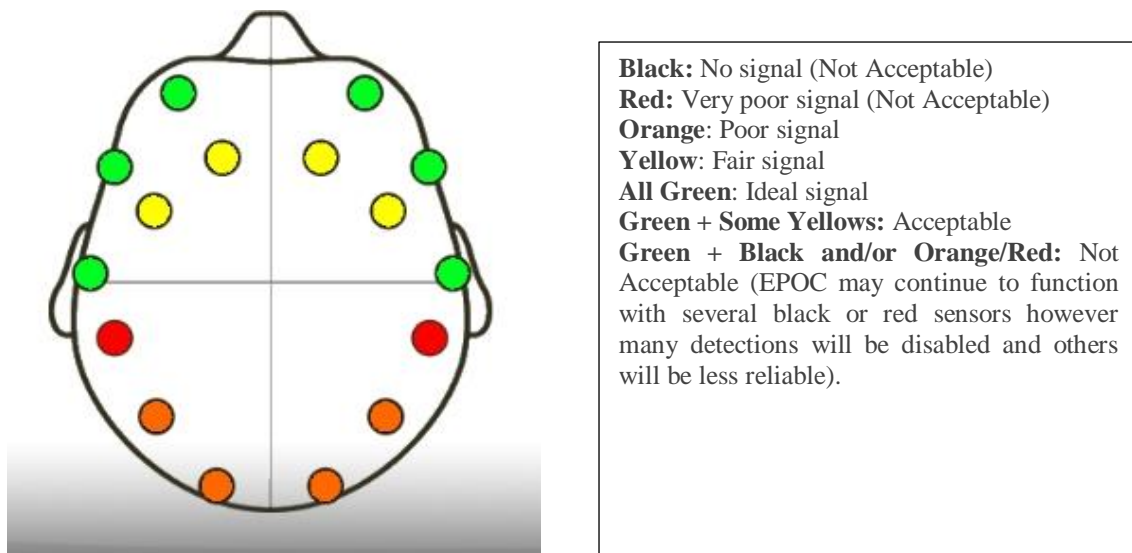
### 3.2 EMOTIV EPOC + SOFTWARE: TEST BENCH

The test bench is composed by the following tabs:

**EEG:** The function of this panel is to display contact quality feedback for the EPOC Neuroheadset’s sensors and guidance to the user the EPOC Neuroheadset correctly. It is

most important for the user to test the contact quality before proceeding to the other EPOC Control Panel tabs. Poor contact quality will result in poor Emotiv detection results, although the EPOC will continue to perform moderately well with a small number of missing or lower quality sensors (Fig.3-2).

Each circle represents one sensor and its approximate location when wearing the SDK headset. The color of the sensor circle is a representation of the contact quality. To achieve the best possible contact quality, all of the sensors should show as green.

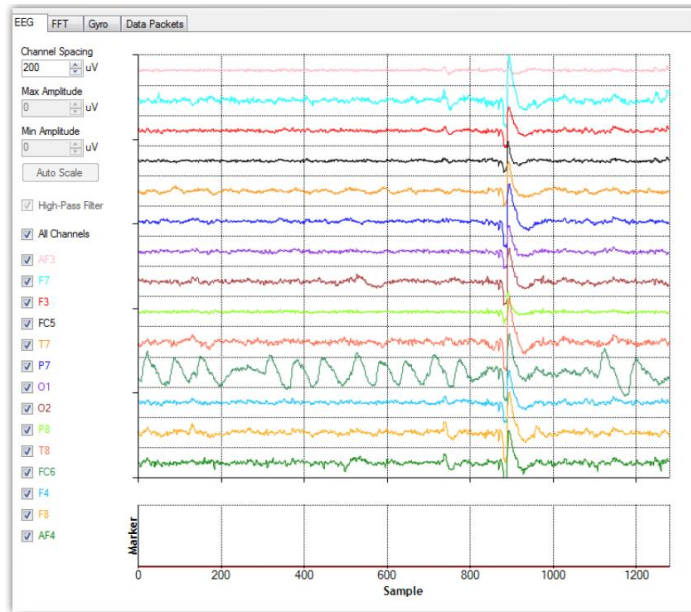


*Figure 3-2 Display of the electrodes contact quality*

Another graph displays the signals from the EEG channels (Fig. 3-3).

It shows brainwave signals of 14 channels (AF3, F7, F3, FC5, T7, P7, O1, O2, P8, T8, FC6, F4, F8, AF4). In this mode, the users can select to display one or different channels.





*Figure 3-3 EEG Channels*

**FFT:** The FFT Suite shows EEG graph in the frequency domain and the power of signal in the frequency band (Fig. 3.4).

The first panel shows the FFT graphs of the selected channel in real time. The second panel displays the power of signal in specific frequency bands: Delta (1-4Hz); Theta (4-7Hz); Alpha (7-13Hz); Beta (13-30Hz).

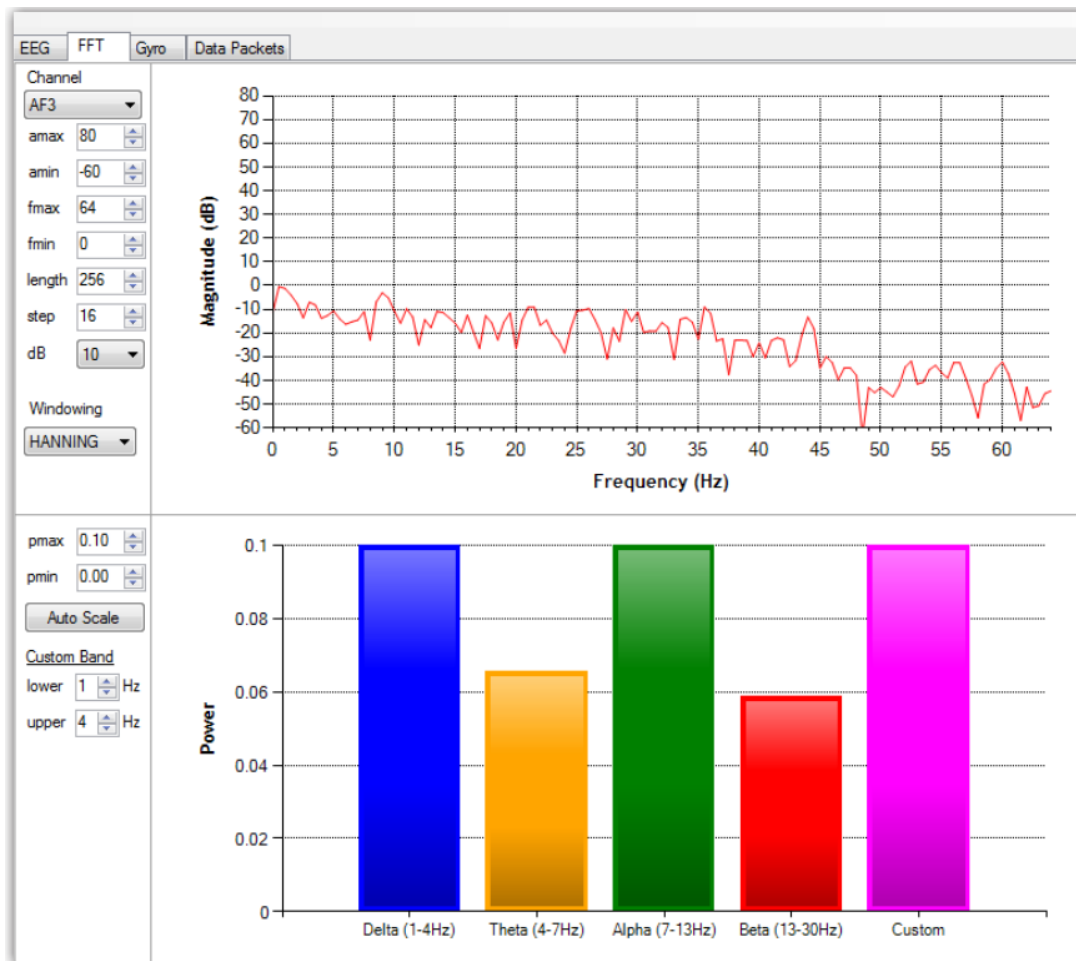


Figure 3-4 FFT EEG Band

### 3.3 EMOTIV EPOC + 3D BRAIN ACTIVITY MAP

This tool displays a real-time map of mental activity in different brainwave frequency bands. Adjustable gain allows you to see detailed information and relative strengths between different brain regions. Adjustable buffer size allows you to see instant responses or average over longer periods.

The Advanced Suite allows to display significant brainwave in any frequency band.

In Fig.3-5 the screen displays brain activity in four significant brainwave frequency bands

(Delta, Theta, Alpha, Beta) and the contact quality for each EPOC sensor.

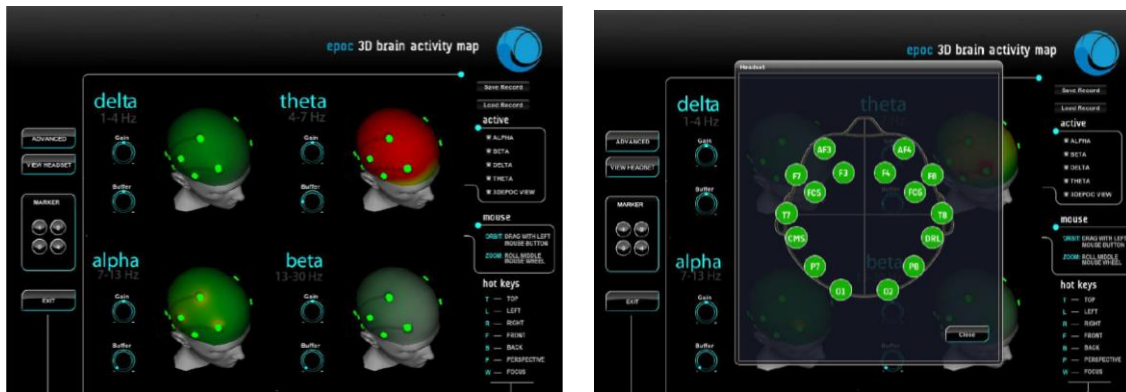


Figure 3-5 Brain activity map



Figure 3-6 Brain Activity summary

Fig 3-6 shows the brain activity in any frequency band defined by the user and the review of a recorded session at any time.

### 3.4 EPOC-SIMULINK CONNECTION

Simulink is a MATLAB [79] environment used to simulate and model dynamic systems.

Simulink supports the simulation of non-linear systems that operate with continuity classifying them based on the continuous or discrete time.

Moreover, Simulink offers a graphic interface that allows to define and create the model through its flowchart. The blocks can be moved. This environment includes an elevated number of libraries that include a wide range of blocks able to develop (easier) operation on the signals. In addition, Simulink integrates itself completely with MATLAB.

In this project, Simulink has been interfaced both with EMOTIV and with MATLAB as explained hereafter.

Simulink can be connected with EMOTIV EPOC + to allow recording in real time EEG signals, synchronizing them with other procedure. By inserting the USB receiver of the Emotiv device and clicking on Epoc-SimulinkSignalserver.exe, the connection is activated when clicking START, as shown in Fig. 3-7.



*Figure 3-7 EPOC Simulink Signal Server*

Then, opening the MATLAB directory by importing the Epoc Simulink Signals folder, the Simulink model opens (Fig. 3-8).

Simulink is an environment for the modeling, the analysis and the simulation of dynamic systems.

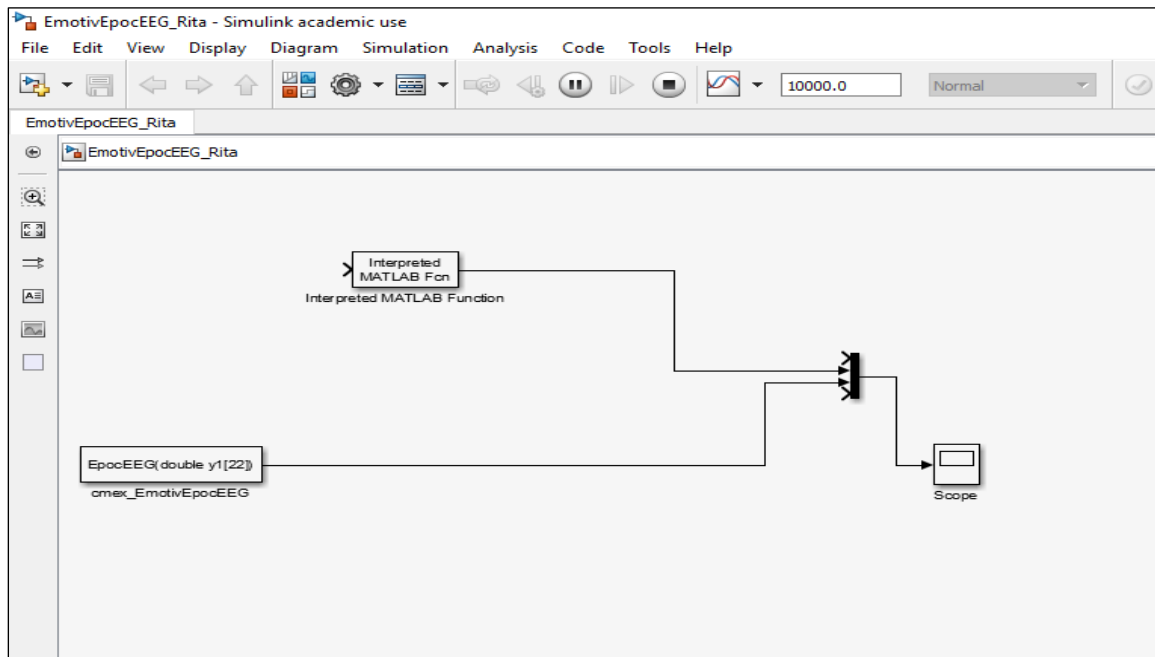
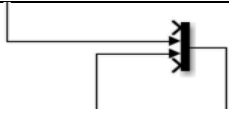
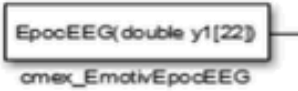



Figure 3-8 The Simulink blocks

The model is formed of a series of blocks that are copied from a library in the work area to create the chosen calculation model (Table 1):

TYPES OF BLOCKS	DESCRIPTION
	<p>This represents the connection of the circuit and is can be seen how all the blocks are connected.</p>
	<p>EpoceEEG real time data synchronization with video frames</p>
	<p>This block receives the data which in real time are converted into numbers.</p>

*Table 1 Types of Simulink blocks with description*

The blocks are graphically connected with oriented links.

When clicking on Run on the blocks window, both the stimulating video and the recording of the signals start in a synchronous mode.

### 3.5 3D EXCELVAN GLASSES

To isolate the sensitive experience of the videos in the surrounding environment we used special glasses connected to the pc.

The 3D EXCELVAN glasses are in general used as Multi-media player for movies, music, photos and books (Fig. 3-9).

The EXCELVAN glasses work with MP4, MP5, PMP, DVD and other multi-media formats.

This Virtual Screen is equipped of detachable earphones, super dynamic quality stereo sound effect. They are endowed with built-in rechargeable battery, advanced micro displays technology, connected to the PC via HDMI .



Figure 3-9 3D-Excelvan Glasses

### 3.6 SELECTED ELECTRODES

In anatomy, the brain is divided into four lobes, differentiated by their location and functions [80].

The electrodes have been selected on the of their functional role in relationship with the chosen electrodes: **F7 (Frontal lobe)**, **T8 (Temporal lobe)**, **P7(Parietal lobe)**, **O1 (Occipital lobe)**.

**F7 (Frontal lobe):** The frontal lobe is the biggest lobe in the brain and the most important lobe for the human species. In anatomy it extends from the frontal pole to the central

sulcus and is composed by different parts: precentral gyrus, premotor cortex, supplementary motor cortex, frontal eye field and motor speech area (Broca speech area)

The association cortex of the frontal lobe, also known as the prefrontal cortex, is a late-developing region of the neocortex. In the human adult, the frontal lobe constitutes as much as nearly one-third of the totality of the neocortex. The most general executive function of the lateral prefrontal cortex is the temporal organization of goal-directed actions in the domains of behavior, cognition, and language.

**T8 (Temporal Lobe):** The temporal lobe is located between the lateral fissure on both cerebral hemispheres, inferior to the lateral sulcus, which separates the frontal lobe and the parietal lobe. The temporal lobe is composed by: superior temporal gyrus, middle temporal gyrus, inferior temporal gyrus, auditory tract, primary auditory cortex, secondary auditory cortex. This lobe is active in processing sensory input and the in the appropriate retention of visual memory, language comprehension, and emotion association.

**P7 (Parietal Lobe):** The parietal lobe is superior to the occipital lobe and temporal lobe, separated from the frontal lobe by the central sulcus. This lobe is composed to: MT middle temporal area postcentral gyrus, primary somatosensory cortex, secondary somatosensory cortex, supramarginal gyrus and angular gyrus. This lobe integrates sensory information among various modalities, including spatial sense and navigation (proprioception). The major sensory inputs from the skin (touch, temperature, and pain receptors), relay through the thalamus to the parietal lobe. Several areas of the parietal lobe are important in language processing.



**O1 (Occipital Lobe):** The occipital lobe is the visual processing center, containing most of the anatomical region of the visual cortex. The primary visual cortex is the Brodmann area 17, and it is located on the medial side of the occipital lobe within the calcarine sulcus; the full extent continues onto the posterior pole of the occipital lobe. This lobe is specialized for different visual tasks, such as visuospatial processing, color differentiation, and motion perception.

We chose in particular to process four electrodes (T8, P7, O1, F7) as the most interesting in relationship with the chosen stimulations. In fact, F7 is involved in cognitive control, T8 in language and visual input and memory, P7 in visuospatial processing and the O1 main functional area is the primary visual cortex. The frequency analyzed were Beta (between 12.5 and 30 Hz) and Gamma (>30 Hz) (Tables 2 and 3).


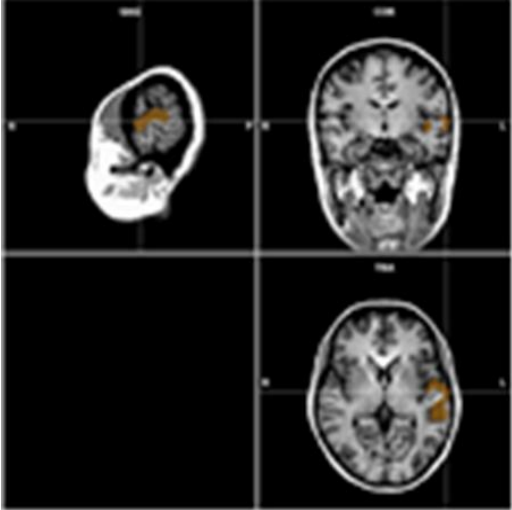
F7	T8
<p><b>Location:</b> Frontal lobe, Rostral region of superior frontal gyrus</p> <p><b>Function, Connectivity:</b></p> <p>BA9 and BA11 make up prefrontal cortex, Executive functions Cognitive control</p> 	<p><b>Location:</b> Temporal lobe</p> <p><b>Function, Connectivity:</b></p> <p>Posterior part contains Wernicke's Area</p> <p>Language comprehension</p> 

Table 2 Selected electrodes F7 (Frontal Lobe) and T8 (temporal lobe)

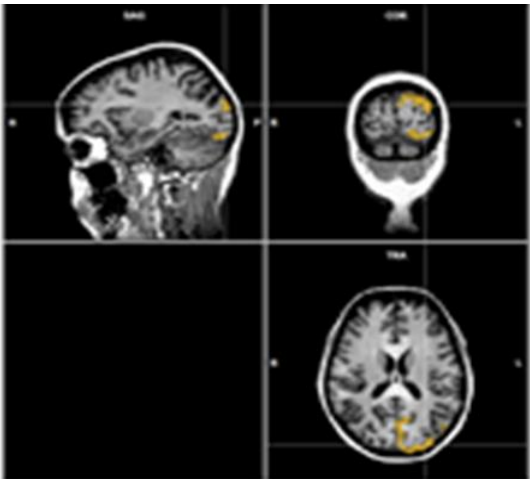
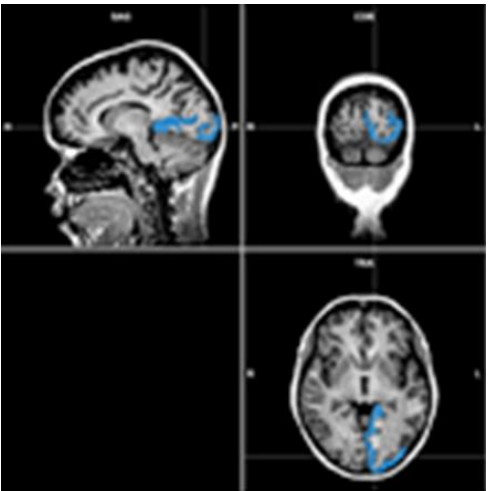
P7	O1
<p><b>Location:</b></p> <p>Occipital lobe</p> <p>Includes parts of cuneus, lingual gyrus and the lateral occipital gyrus</p> <p><b>Function, Connectivity.</b></p> <p>Visual processing</p> 	<p><b>Location:</b></p> <p>Medial part of occipital lobe</p> <p><b>Function, Connectivity.</b></p> <p>Initial site of cortical processing of visual information</p> <p>Organized in orientation columns,</p> 

Table 3 Selected electrodes P7 (parietal Lobe) and O1(Occipital Lobe)

## 3.7 VIDEOS

We created two videos representing different perceptions and cognitive stimuli.

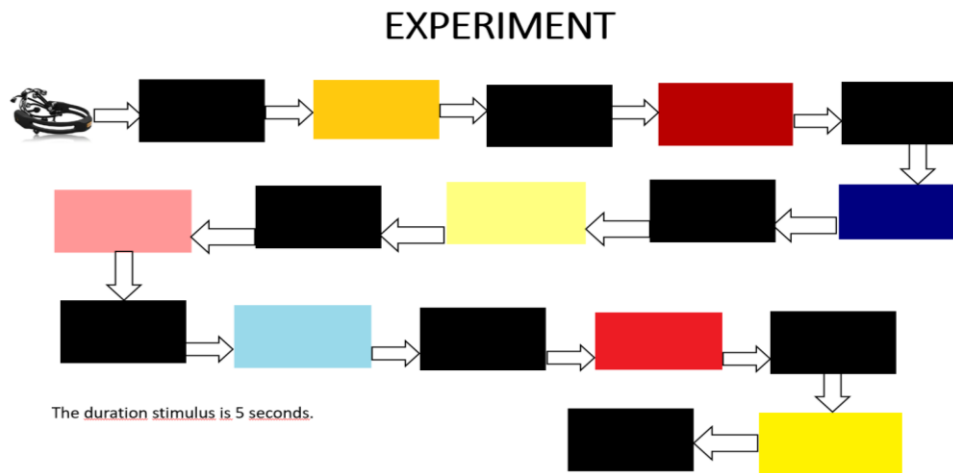
The videos have been realized with PowerPoint. Successively the Power Point presentation has been saved into .mp4 format and synchronized using the Simulink procedure.

### 3.7.1 First Colors Test

The First Colors test consists of three tones of the same colors. The colors that have been selected are: Yellow, Red and Blue. Each colored stimulus last 5 s and is followed by a 5 s black stimulus, as a function of control and reset (Table 4 and Fig. 3-10).

COLORS	LIGHT COLORS	DARK COLORS
<p><i>YELLOW</i></p> 		
<p><i>RED</i></p> 		
<p><i>BLU</i></p> 		

*Table 4 First Colors test*












*Figure 3-10 The first Colors test*

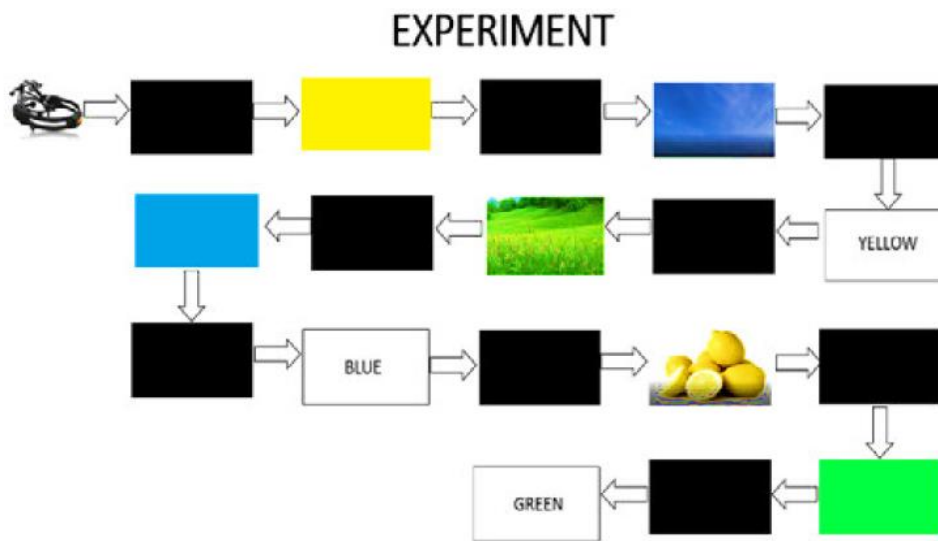
### 3.7.2 Second Colors test

In this test we selected: colors, color imagines recalling colors written words representing colors and sounds of the words of the colors.

The stimuli last 5s, followed by a 5 s black stimulus, as a function of control and reset (Table 5 and Fig. 3-11).

COLORS	COLORED IMAGES	WRITTEN COLORS	COLORS SOUND
<p><i>YELLOW</i></p> 	<p><i>LEMONS</i></p> 	<p><b>YELLOW</b></p>	 <p><i>YELLOW</i></p>
<p><i>GREEN</i></p> 	<p><i>MEADOW</i></p> 	<p><b>GREEN</b></p>	 <p><i>GREEN</i></p>
<p><i>BLUE</i></p> 	<p><i>SKY</i></p> 	<p><b>BLUE</b></p>	 <p><i>BLUE</i></p>

*Table 5 Second Colors Test*



*Figure 3-11 The second Colors test*

### 3.8 EXPERIMENTAL PROCEDURE

We collected 10 recordings from eight men and two women, aged between 22 and 65; the educational level was graduations and PhD (Table 6).

The above described Simulink procedure synchronizes the acquired signals with the various sensory and cognitive experiences presented in the videos. At the end of the experiment, signals are recorded and the analysis procedure is applied.



<b>SEX</b>	<b>AGE</b>	<b>EDUCATION LEVEL</b>
<i>8 MEN</i>	<i>22-65</i>	<i>Master Degree.</i>
<i>2 WOMEN</i>	<i>30-60</i>	<i>Master Degree.</i>

*Table 6 Subjects Data*

## 4 SIGNAL PROCESSING

### 4.1 EMOTIVE EPOC +: DATA PRE-PROCESSING

The EMOTIVE EPOC + system provides data to the user at a sampling rate of 128 Hz, although per the technical specifications it works at a rate of 1024 Hz internally. The down sampling is for various technical reasons including wireless transmission to the receiver. Resolution is approximately 0.5 microvolts (14 bits). The working bandwidth is 0.2 to 43 Hz, allowing recordings into the low gamma range, and there are notch filters at 50 and 60 Hz for 7 electrical noise in both North America and Europe (Fig. 4-1).

<p><b>Signals</b></p> <ul style="list-style-type: none"><li>• 14 channels: AF3, F7, F3, FC5, T7, P7, O1, O2, P8, T8, FC6, F4, F8, AF4</li><li>• 2 references: In the CMS/DRL noise cancellation configuration P3/P4 locations</li></ul> <p><b>Signal resolution</b></p> <ul style="list-style-type: none"><li>• Sampling method: Sequential sampling. Single ADC</li><li>• Sampling rate: 128 SPS or 256 SPS* (2048 Hz internal)</li><li>• Resolution: 14 bits 1 LSB = 0.51<math>\mu</math>V (16 bit ADC, 2 bits instrumental noise floor discarded), or 16 bits*</li><li>• Bandwidth: 0.2 - 43Hz, digital notch filters at 50Hz and 60Hz</li><li>• Filtering: Built in digital 5th order Sinc filter</li><li>• Dynamic range (input referred): 8400<math>\mu</math>V(pp)</li><li>• Coupling mode: AC coupled</li></ul>
---

*Figure 4-1 From the Epoc+ manual: Epoc+ parameters*

The online EEG was sampled at 1000 Hz with an online bandpass filter from 1 to 100 Hz. The signals from the other 14 scalp sites (channels) were high-pass filtered with a 0.16 Hz cut-off, pre-amplified and low-pass filtered at an 83 Hz cut-off. The digitized signal was filtered using a 5th-order sinc notch filter (50–60 Hz), low-pass filtered and down-sampled to 128 Hz.

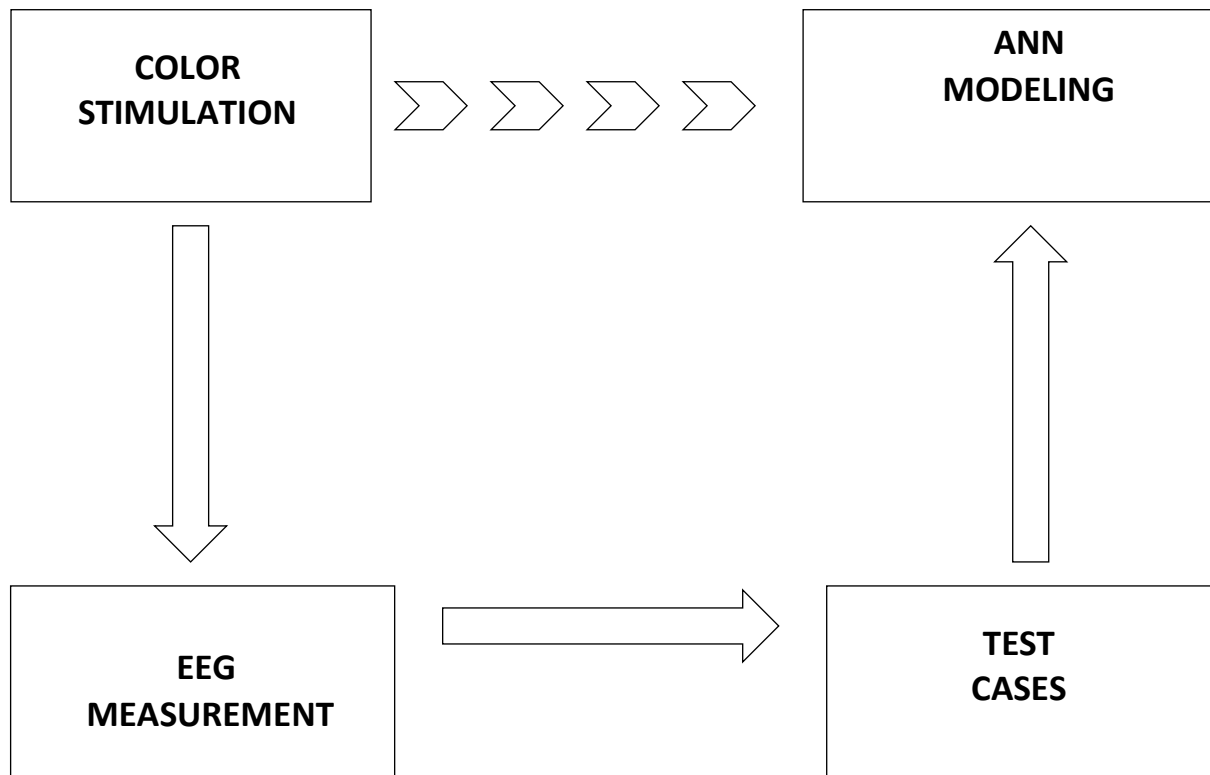
The system provides an embedded, in signals processing, a sinc filter is an idealized filter that removes all frequency components above a given cutoff frequency, without affecting lower frequencies, and has linear phase response. It is an "ideal" low-pass filter in the frequency sense, perfectly passing low frequencies, perfectly cutting high frequencies; and thus may be considered to be a *brick-wall filter*.

Real-time filters can only approximate this ideal, since an ideal sinc filter (a.k.a. *rectangular filter*) is non-causal and has an infinite delay, but it is commonly found in conceptual demonstrations or proofs, such as the sampling theorem and the Whittaker–Shannon .

## 4.2 PROCESSING

As previously presented, the aim of this work is that of using the EEG tracing to isolate some sensorial and cognitive stimuli (colors, writings or words) comparing the resulting attractors and maximizing the similarities between similar stimuli and the differences between different stimuli. For this reason, we used the ANN ITSOM network.

The parameters of the neural network have been optimized during the analysis. A schema of the ideal structure of the whole system can be depicted as in Fig. 4-2 .



*Figure 4-2 System representation. The dotted line indicates the ideal correspondence between the neural correlates of color perception and the ANN attractors.*

The full tracing has been cleared from the start and end columns leaving only the 14 columns deriving from the electrodes.

The file has been further filtered through two elaboration chains written in MATLAB to separate and distinguish beta and gamma frequencies.

- **butterbeta.m** (Butterworth band-pass filter between 14 and 30, beta waves)
- **buttergamma.m** (Butterworth band-pass filter between 31 and 46, gamma waves)

The procedures create two filtered files in beta and gamma frequencies for all the electrodes. A track that divides the sampled signal compared to the different stimulations is included in a script that creates one file (**blue.txt, yellow.txt, ecc.**) for each stimulation.

The electrodes in each file are in the following order:

**AF3, F7, F3, FC5, T7, P7, O1, O2, P8, T8, FC6, F4, F8, AF4.**

At the end, for each stimulation we have: 4 filtered files, one for electrode **F7, P7, O1, T8**. Therefore, there are 8 unidimensional files in total, relating to each individual color/writing/voice stimulation.

### 4.3 ITSOM APPLICATION

The sampled amplitudes files, thus divided, are elaborated by the ANN which is written in C ANSI.

The ITSOM network is able to process more signals simultaneously but in this case it was useful to process one signal at a time.

Starting parameters selected to elaborate this kind of signal are summarized in Table 7. However, these parameters have been modified from time to time until a dynamic stabilization threshold is reached.

<b>INPUT NEURONS</b>	1500
<b>COMPETITIVE LAYER NEURONS</b>	15 neurons
<b>LEARNING RATE</b>	0.01
<b>DELTA1</b>	0
<b>DELTA2</b>	0
<b>NUMBER OF EPOCHS</b>	400

*Table 7 Initial parameters for ITSOM*

The executable creates four output files in a subfolder that contain the signal files:

**DYNDEC.txt, WEIGHTS.txt, ZSCORE.txt, ZREALS.txt**

**DYNDEC.txt:** Represent the winning neurons that is those neurons that win the competitions with weights. Fig. 4-3 shows a typical series of winning neurons.

7  
3  
8  
7  
3  
8  
7  
5  
3  
8  
7  
11  
5  
3  
8  
7  
11  
5  
3  
8  
10  
7  
9  
11  
5  
3  
8  
10  
7  
9  
11  
5  
3  
8  
10  
7  
9  
11  
5  
3  
8  
10  
7  
9  
11  
5  
3  
8  
6  
7  
10  
9  
11  
5

*Figure 4-3 Series of winning neurons of the yellow stimulation on electrode F7*

## WEIGHTS.txt :The weights are visualized with the goal of perform a control on their variation (Fig. 4-4).

The image shows a Notepad++ window with a file named "pesait - Blocco note". The window displays a large grid of numerical data, which are weights from an ANN. The data is organized in approximately 20 columns and 40 rows. Each row starts with a label "nuovo strato" followed by a series of numerical values. The values are floating-point numbers, some with many decimal places, representing the weights of the neural network at different stages of evolution.

Figure 4-4 Snapshot of the weights variation file, indicating the ANN evolution in the time

## ZREALS.txt: Coding in real numbers without threshold (Fig. 4-5).

0.082171	-0.183868	-0.301327	-0.301327	0.135981	-0.047335	-0.301327	-0.200935	0.580618	0.537449
0.104354	0.045320	-0.194397	-0.357786	-0.357786	-0.338108	0.035182	0.607043	0.457370	-0.001193
-0.098120	-0.158229	-0.009724	0.079557	0.155578	0.380988	0.551593	0.074253	-0.445518	-0.530378
-0.206759	-0.206759	-0.206759	-0.203661	0.174891	0.281574	0.806386	-0.101108	-0.206759	-0.131048
0.214310	0.133591	0.447724	0.007130	-0.403867	-0.403867	0.311174	0.317901	-0.220230	-0.403867
-0.359849	-0.226727	0.097683	0.233803	0.153450	0.329746	0.613380	-0.219531	-0.359849	-0.262106
0.261997	-0.272250	-0.070558	0.709226	-0.329587	-0.397717	-0.116428	0.210731	0.112920	-0.108333
-0.168074	-0.168074	-0.168074	-0.153785	-0.168074	-0.168074	-0.138096	0.299529	0.852024	-0.019304

Figure 4-5 List of Z real numbers



**ZSCORE.txt** : after the application of the threshold, the zeta score code processes in a binary string the dynamic behavior (Fig. 4-6).

```

0 0 0 0 0 0 0 1 0 0
0 1 0 0 0 1 1 1 0 0
0 0 0 0 0 1 1 1 0 0
0 0 0 0 0 1 1 1 0 0
0 0 0 0 0 1 1 1 0 0
0 0 0 0 0 0 0 1 0 0
0 0 0 0 0 0 0 1 0 0
0 1 0 0 0 1 1 1 0 0
0 1 0 0 0 1 1 1 0 0
0 0 0 0 0 1 1 1 0 0
0 0 0 0 0 0 0 1 0 0
0 1 0 0 0 1 1 1 0 0
0 0 0 0 0 1 1 1 0 0

```

*Figure 4-6 0s and 1s sequence that represents the network dynamic behavior*

Once these files are generated, it is verified if the zscore are (as much as possible) similar for similar stimuli and different for different stimuli.

If this is not the case, we look at zreal and see if, changing the delta threshold between 0 and 1, the zscore would change in a more appropriate way. In this situation, the threshold is changed.

Otherwise, we proceed to change the other parameters of the network and restart the procedure. As a general rule, larger competitive layers make it more difficult to find correspondences. The learning rate should move the weights of the network at every epoch, but not too much because the network must remain stable. If the weights do not move, Dyndec.txt gives a series of equal values or close to equal. Dyndec.txt should show groups of numbers that, more or less, repeat themselves in time. In the first epochs there could be a transient, then the network should stabilize itself. It might tend to move and show new numbers, but it should not change completely. The optimization of the

parameters should at the end be a single one for all the elaborated signals.

#### 4.3.1 ITSOM RESULTS

In this paragraph the optimized ITSOM parameters and the results are presented (Table 8).

<b>INPUT NEURONS</b>	<b>500</b>
<b>COMPETITIVE LAYER NEURONS</b>	<b>10</b>
<b>LEARNING RATE</b>	<b>0.001000</b>
<b>DELTA1</b>	<b>-0.200000</b>
<b>DELTA2</b>	<b>0.200000</b>
<b>NUMBER OF EPOCHS</b>	<b>150</b>

*Table 8 Optimized ITSOM parameters*

#### 4.3.2 First Colors Test Results

In Table 9 are reported the tones of colors that have been mainly involved, considering all the available recordings, and on which electrode they have had an impact on the presence of the chaotic attractor. Light yellow and dark yellow are present both on F7 and T8 electrodes. The O1 electrode did not detect any correlation.

We highlight these results, divided in stimulation and reference electrodes.

COLORS TONES	ELECTRODES
LIGHT BLUE  DARK BLU  LIGHT YELLOW  DARK YELLOW	F7
RED  PINK	P7
LIGHT YELLOW  DARK YELLOW	T8

*Table 9 First Colors test: highest correlation between stimuli and electrodes*

In the Table 10 are reported, for each stimulus and electrode, the corresponding binary code. The EEG band the results refer to is the gamma band, since the beta band did not present satisfying results. The table refers to the best recording available.

STIMULI	ELECTRODES	BINARY CODE
BLUE	F7	1 0 1 1 0 0 0 0 0 1
DARK BLU		1 0 1 1 0 0 0 0 0 0
LIGHT YELLOW		1 0 1 0 1 0 0 0 0 0
DARK YELLOW		1 0 1 0 1 0 0 0 0 0
DARK RED	P7	0 0 0 0 0 1 1 1 1 0
RED		0 0 0 0 1 1 1 1 1 0
LIGHT YELLOW	T8	0 1 0 1 1 1 1 1 0 0
DARK YELLOW		0 1 0 1 0 1 0 1 0 0

*Table 10 Stimulus, Electrode and corresponding binary Code: best similarities*

It can be deduced that similar stimuli have similar responses and different stimuli have different codes.

#### 4.3.3 Second Colors Test Results

The second colors test consists of the presentation of colored stimuli with different features entities such as: monochromatic, color associated to pictures, written colors and in audio format. As in the previous example, Table 11 shows what are the images, colors, colored writings that have been mainly involved in relation to which electrodes. In this case the electrodes that showed the highest involvement in the stimuli were F7 and O1.

STIMULI	ELECTRODES
WRITTEN GREEN WRITTEN MEADOW SKY WRITTEN SKY	O1
WRITTEN GREEN WRITTEN MEADOWN SKY WRITTEN SKY YELLOW SOUND WRITTEN YELLOW YELLOW WRITTEN LEMON MEADOW SOUND GREEN WRITTEN YELLOW SOUND YELLOW IMMAGIN COLORS LEMON SOUND MEADOWN SOUND LEMON WRITTEN YELLOW	F7
LIGHT BLUE SKY WRITTEN LIGHTBLUE	T8
YELLOW LEMONS WRITTEN YELLOW	
GREEN MEADOW WRITTEN GREEN	

Table 11 Second Colors test: highest correlation between stimuli and electrodes

A common element on the four electrodes is that there is a higher involvement of the colors when in written form. As in the previous experiment, the results displayed are related to the gamma band, since the beta band did not report significant results.

Hereafter (Table 12) are summarized the stimuli, electrodes and bands involved with binary codes. Also in this case it is confirmed that similar stimuli offer similar binary codes.

<b>STIMULI</b>	<b>ELECTRODES- EEG BAND</b>	<b>BINARY CODE</b>
LIGHTBLUE SKY WRITTEN LIGHTBLUE	T8 GAMMA	0 0 0 1 1 0 1 0 1 0 0 0 0 1 1 0 0 1 1 0 0 0 0 1 1 0 1 1 1 0
YELLOW LEMONS WRITTEN YELLOW		1 0 0 1 0 0 1 1 1 1 1 0 0 1 0 0 1 1 1 1 1 0 0 0 0 1 1 1 1 1
GREEN MEADOW WRITTEN GREEN		0 0 0 0 0 1 0 1 0 0 0 0 0 0 0 1 1 1 0 0 0 0 0 0 0 1 1 1 0 0
YELLOW LEMONS WRITTEN YELLOW	P7 GAMMA	1 0 0 0 0 1 0 0 1 1 1 0 1 0 0 0 1 1 1 0 1 0 1 0 0 0 1 1 0 0
LIGHT BLUE WRITTEN LIGHTBLUE		0 1 0 0 0 0 1 1 0 0 0 0 0 0 0 0 1 1 0 0
WRITTEN GREEN MEADOW SOUND	F7 GAMMA	0 0 0 0 0 0 1 1 0 0 0 0 0 0 0 0 1 1 0 0
WRITTEN LEMON YELLOW		1 0 0 1 0 0 0 0 0 0 1 0 0 1 1 0 0 0 0 1

YELLOW LEMON SOUND	F7 GAMMA	1 0 0 0 1 0 0 0 0 0 1 0 0 0 0 0 0 1 0 0
WRITTEN YELLOW YELLOW SOUND		1 0 0 0 0 0 1 1 1 0 1 0 0 0 0 0 0 1 1 0
SKY WRITTEN SKY		0 0 0 0 0 0 0 0 0 1 0 0 0 0 1 0 0 0 0 0
WRITTEN GREEN WRITTEN MEADOWN	O1 GAMMA	0 0 0 1 1 0 0 0 1 0 0 0 0 1 1 0 1 1 0 0
SKY WRITEN SKY		0 0 0 0 1 1 0 0 0 0 0 0 0 0 1 0 0 0 0 0

*Table 12 Stimuli, Electrodes and Binary codes of the second Colors test*

#### 4.4 CORRESPONDENCE BETWEEN STIMULI AND SHAPE OF ATTRACTORS

It is important to outline that there is a correspondence not only in the codes, but also in the shape of the attractors during the phases related to the considered stimuli. As we said the attractors are created from the series of the winning neurons, using a two dimensional model.

In Tab. n. 13-14-15 the first column shows the sensory and cognitive stimuli, the second column shows the binary code resulted from the ANN processing the third column shows the attractors generated by the dynamics of the sequence of the ITSOM winning neurons.

We can observe that similar stimuli present attractors that have a similar shape. Moreover, this shape is different from that of the attractors deriving from different stimuli.

The shape of the configuration of these attractors could therefore be apt to represent the qualitative aspect of the states of consciousness, the so-called “*qualia*” [88], [89], [90].

It must be outlined that of course the concept of ‘*qualia*’ refers to a purely subjective phenomenon: it cannot be observed from ‘outside’, is not available by correlative measures or physics in generally. It accounts for the subjective ‘meaning’ of information, not to its contents or the diversity or differences in perception .

Thus we have to stress that in this work we are dealing with a *representation* of the perceptive counterpart of “*qualia*”.




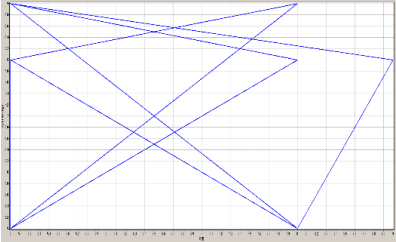

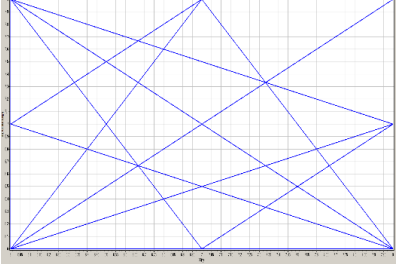
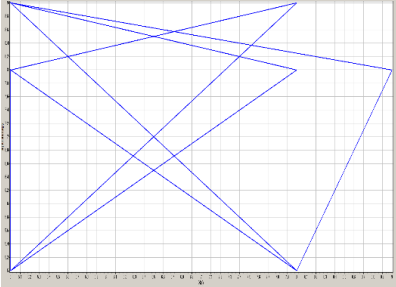
STIMULUS	BINARY CODE	CHAOTIC ATTRACTORS
<p data-bbox="300 412 448 450"><i>YELLOW</i></p> 	<p data-bbox="596 506 890 544"><b>1 1 0 0 1 0 1 1 1 1</b></p>	
<p data-bbox="300 770 448 808"><i>LEMONS</i></p> 	<p data-bbox="596 864 890 902"><b>1 1 0 0 0 0 1 1 1 1</b></p>	
<p data-bbox="300 1223 448 1261"><i>YELLOW</i></p>	<p data-bbox="596 1229 890 1267"><b>1 1 0 0 0 1 1 1 1 1</b></p>	

Table 13 Results of the Yellow stimulus




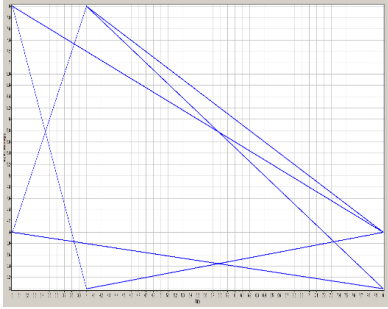
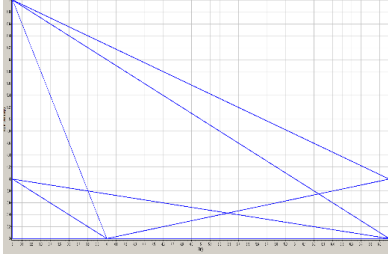
STIMULUS	BINARY CODE	CHAOTIC ATTRACTORS
<p data-bbox="379 405 464 434"><i>BLUE</i></p> 	<p data-bbox="639 595 948 624">0 0 0 1 1 0 0 0 1 0</p>	
<p data-bbox="392 741 451 770"><i>SKY</i></p> 	<p data-bbox="639 931 948 960">0 0 0 1 1 0 1 0 1 0</p>	
<p data-bbox="379 1211 464 1240"><i>BLUE</i></p>	<p data-bbox="639 1312 948 1341">0 0 0 1 1 0 0 1 1 0</p>	

Table 14 Results of the Blue stimulus


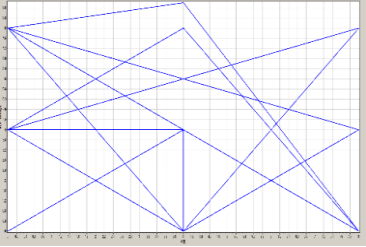

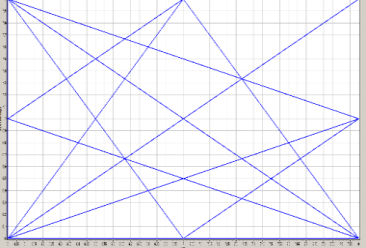
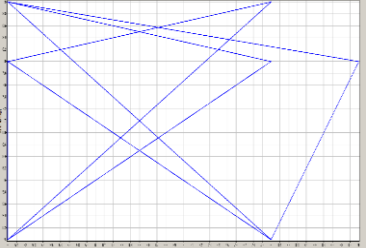
STIMULUS	BINARY CODE	CHAOTIC ATTRACTORS
<p data-bbox="316 405 432 439"><i>GREEN</i></p> 	<p data-bbox="600 595 911 629"><b>0 0 0 0 0 1 1 1 0 0</b></p>	
<p data-bbox="300 719 448 752"><i>MEADOW</i></p> 	<p data-bbox="600 909 911 943"><b>1 0 0 0 0 1 1 1 0 0</b></p>	
<p data-bbox="320 1200 427 1234"><i>GREEN</i></p>	<p data-bbox="600 1207 911 1240"><b>1 0 0 0 0 0 1 1 0 0</b></p>	

Table 15 Results of the Green stimulus

#### 4.5 FINAL RESULTS

From the results of the first observation we can highlight that:

1. The electrode that presents a higher correspondence with the stimulations is T8.

2. Low presence of correspondence relative to pure colors.
3. Substantial absence of spurious correspondences between pure colors or between images,
4. Low correspondence of the red color and similar (red appears with 4 electrodes),
5. Clear higher number of correspondences for writing and words,
6. The stabilization of the network is when reaching 150 epochs and is maintained until over 1200 epochs.
7. The Gamma band shows in both experiments a higher correspondence between binary codes.
8. There is a correspondence between stimulus and shape of the attractor: again. Similar stimuli give rise to similar attractor shapes, different stimuli give rise to different attractor shapes.

## 5 EVALUATION OF INTEGRATED INFORMATION

As mentioned in cap. 1, IIT refers to the mathematical theory of information proposed by C. Shannon and W. Weaver [17]. According to this framework, information is defined as the reduction of uncertainty among a number of possible outcomes  $x$  of a random variable  $X$  when one of them occurs. Thus, an increase of uncertainty corresponds to higher information, and the information content of  $x$ ,  $I(x)$ , will be a decreasing function of its probability. Shannon showed that this function is expressed by

$$I(x) = -\log_2 P(x)$$

where  $P(x)$  is the probability that  $x$  occurs. Entropy of the random variable  $X$  is defined as the expected value of the information content of  $X$  (i.e. its average information content).

$$H(X) = E(I(X))$$

Thus Entropy can be defined as a measure of the uncertainty associated with  $X$ . Given two subsets  $A$  and  $B$  defining a single bipartition of a system  $X$ , Mutual Information measures the uncertainty of  $A$  that is accounted for by the state of  $B$ , and is defined as

$$MI(A; B) = H(A) + H(B) - H(AB)$$

The Effective Information of a system measures the extent to which its repertoire of possible states is differentiated in response to all possible inputs. Effective Information is calculated as the Mutual Information across a partition when the outputs from one subset have maximum Entropy.

As before mentioned, the IIT hypothesizes that consciousness corresponds to the capacity of the system to integrate information, and this measure is indicated by  $\Phi$ .

$\Phi$  is defined as the Effective Information across the weakest link of the system, i.e. the Minimum Information Bipartition. The Minimum Information Bipartition is the partition of the system for which the Effective Information is lowest.

To summarize, in order to calculate the integrated information of a system  $\Phi$  (thus a measure of consciousness, as intended in the IIT framework) it is sufficient to calculate the integrated information between two partitions of the system, among all the possible ones, which have the lesser amount of effective information between them. A high value  $\Phi$  will denote highly structured complexity. In the brain, the thalamo-cortical system can be described as a single large highly complex system whereas, on the contrary, the cerebellum consists of a large number of very small complexes, each corresponding to a single module and thus having a very low complexity. In terms of complexity, the differences between brain and cerebellum are therefore not the amount of effective information related to the repository of possible states that characterize each system, but rather the level of integration of the information contained therein.

Hence the flow of information between two parts of the same system must be considered.

But once defined a formal way to measure  $\Phi$  and once identified a brain system that may represent a good candidate to generate integrated information, a method to represent complexity and integration in brain structures in such a way as to quantify  $\Phi$  from real

data must be developed.

One of the methods currently studied to analyze complexity in brain structures is to study the brain as a dynamical system.

Brain dynamics refers typically to the dynamics of neuronal populations, networks or columns within cortical areas. It is characterized by its high complexity, often involving oscillations at different frequencies and amplitudes, perhaps interrupted by chaotic or pseudo-chaotic irregular behaviour. Synchronization among groups of neurons were first discovered in the olfactory system [81], [82], but has also been demonstrated in other brain structures, such as the hippocampus [83] [84] and the visual cortex [85], [86], where the oscillations tend to synchronize in phase.

Synchronous oscillations can occur in nearby neurons, but also over considerable distances across spatially separate columns [86] and even between cortical areas [85], [87]. According to IIT, several aspects of the organization of the cortico-thalamic system and of transient attractor dynamics appear well suited to information integration.

It has been recognized that the massive interconnectivity within and among cortical areas (and with thalamus) provides an ideal substrate for cooperative dynamics among distributed neurons [88]. A plausible scenario for characterizing such dynamics is in terms of *transient attractors*.

In fact neurons in the cortico-thalamic system seem to behave in such a way as to ensure the rapid emergence of firing patterns that are distributed over wide regions of the cortex, where some neurons are strongly activated, and many more are deactivated. These firing patterns remain stable (hence they form attractors) over a time scale of tens/hundreds of milliseconds, but then rapidly dissolve (hence the attractors are transient), to make room for another transient attractor.

Attractors have been indicated in the form of binary strings (e.g. in a Hopfield network

consisting of 8 elements with 6 embedded attractors, the attractors are indicated with 00001111, 00110011, 01010101, and their mirror images.)

Metastable systems, namely dynamical configurations that constitute non-fixed-point attractors, are good candidates to form a class of systems with high  $\Phi$  [89], [90], [91].

Our approach stems from the wide literature mentioned above. With the ANN ITSOM, we show how the dynamical analysis of neural signals may highlight the existence of chaotic attractors, differentiated depending on the cognitive states, that outlines the attractors in which the corresponding dynamical system is evolving.

If the attractors show to be chaotic, this means that the neural signals are individually self-organized and, when analyzing more signals together, that there is a form of coherence between signals. The ANN can also highlight the time course of this form of coherence and identify different attractors with a unique code as we have the ANN allows to attribute the same codes to similar but not identical brain events, reaching the necessary range of flexibility. In Table 12 the first columns show the sensory and cognitive stimuli, the second columns show the binary code resulted from the ANN processing, the third columns show the attractors generated by the dynamics of the sequence of ITSOM winning neurons: the figure represents a snapshot of movies that show a typical chaotic path.

To summarize the results, comparing the stimuli, the codes in Table 16 are obtained, clearly highlighting how similar stimuli give rise to similar codes, that result to be quite different from the codes obtained by different stimuli.



<b>YELLOW -&gt; 1100101111</b>	<b>LIGHT BLUE -&gt; 0001101010</b>	<b>GREEN-&gt; 1000011100</b>
<b>LEMONS-&gt; 1100001111</b>	<b>SKY -&gt; 0001100010</b>	<b>MEADOW-&gt; 0000011100</b>
<b>WRITTEN YELLOW -&gt; 1100001111</b>	<b>WRITTEN LIGHT BLUE -&gt; 0001100110</b>	<b>WRITTEN GREEN -&gt; 1000001100</b>

Table 16 Summary of the results. Codes of similar stimuli are similar, codes of different stimuli are quite different

## 5.1 INTEGRATED INFORMATION CALCULUS

In order to quantify the IIT content of the organized signals collected after perceptive and cognitive stimulations we considered the case of the T8 electrode in gamma band, that showed the best results in the previously described analysis.

Using the tool available at the website of the Center of Sleep and Consciousness of the University of Wisconsin [92] [93], that implements the procedure explained at the paragraph 1.2, we have been able to calculate the  $\Phi$  value of the specific patterns through their related dynamical attractors.

The summary of results is sketched in Table 17, where  $\Phi$  represents the integration at a system level.

The dynamical representation in the concept (*qualia*) space of some of the patterns is reported in Figures 5-1, 5-2, 5-3, and their conceptual structure after calculation in the IIT framework is depicted in Figures 5-4, 5-5, 5-6.

Pattern	$\Phi$
YELLOW	0.08323
BLUE	0.08323
GREEN	0.21528
LEMON	0.21528
SKY	0.08323
MEADOW	0.21528
WRITTEN YELLOW	0.21528
WRITTEN BLUE	0.21528
WRITTEN GREEN	0.21528

Table 17 Integrated Information Calculus

In conclusion, for all the color stimulations the  $\Phi$  value was equal to 0.08323, except for the Green color that had a  $\Phi$  value equal to 0.21528. The other stimulations had a  $\Phi$  value higher than the pure colors and equal to 0.21528: in line with the IIT, this is correct as they have not only sensory but also cognitive contents, thus should involve more neural structures and can be considered more complex. Although the  $\Phi$  value of stimulation patterns of information content with equivalent complexity coincide, their specific information contents are diverse and composed by subsystems with different values.

We would be tempted to state that these codes can be a way to identify *qualia*, i.e. the subjective and qualitative experience of mental conscious states and of their neural correlates [91], as there is an extremely high number of possible binary codes, but we can distinguish a set of dynamical states with unique codes that we may call “*qualia* codes”.

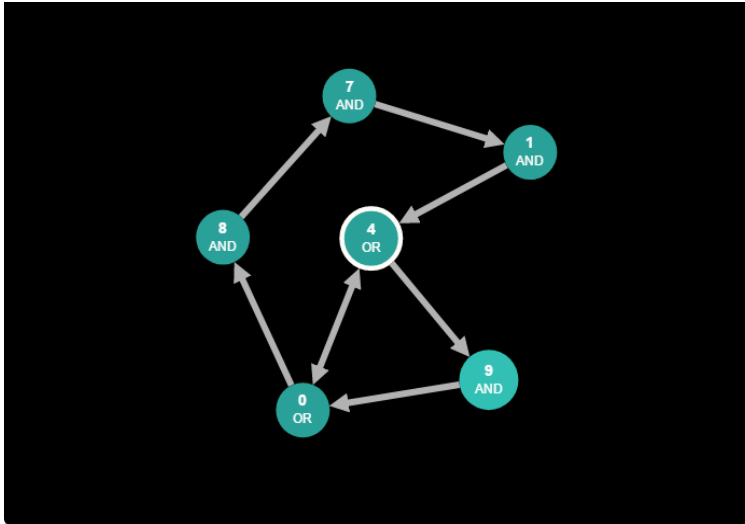


Figure 5-1 Attractor of Yellow

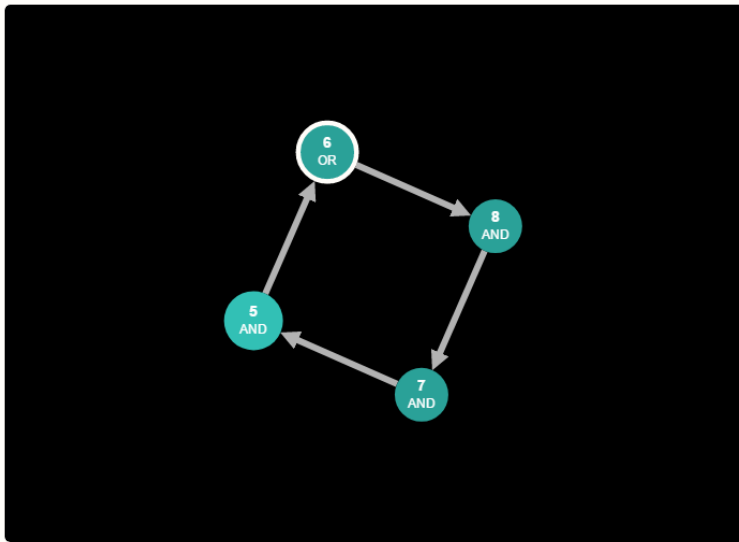


Figure 5-2 Attractor of Lemon

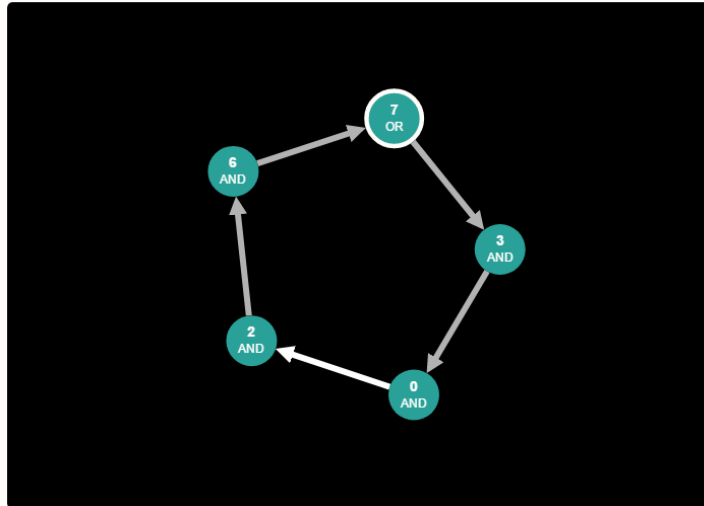


Figure 5-3 Attractor of Written Green

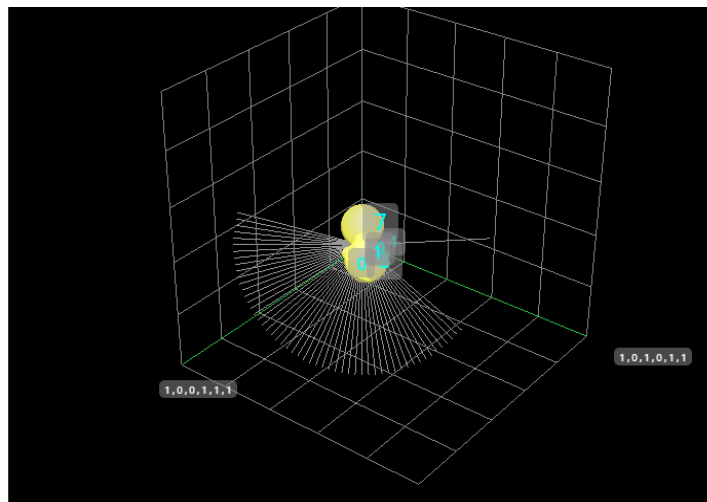


Figure 5-4 Conceptual structure of Yellow

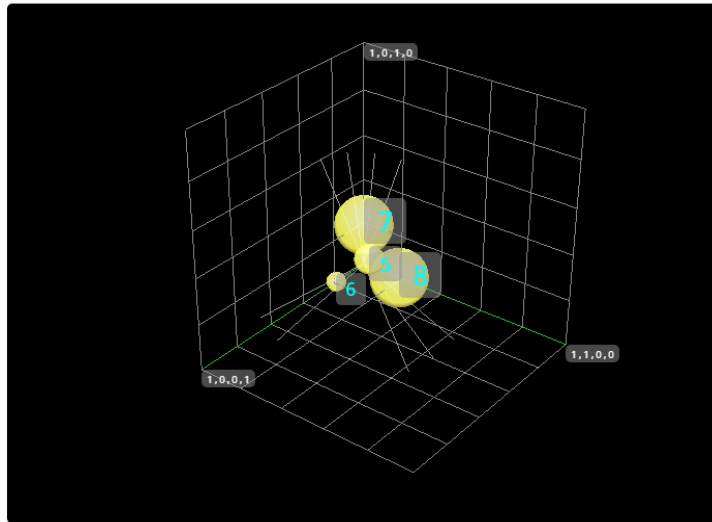


Figure 5-5 Conceptual structure of Lemon

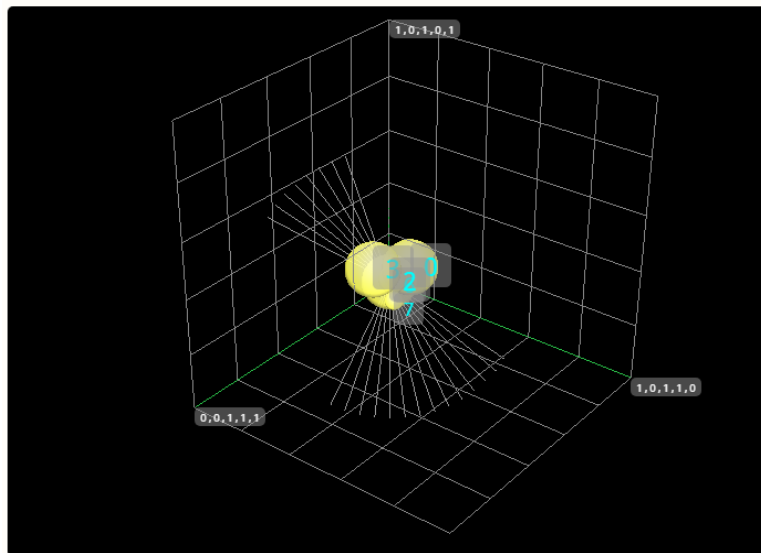


Figure 5-6 Conceptual structure of written Green

## 6 CONCLUSION

The aim of this thesis was the development of a method for the identification of perceptive and cognitive mental states starting from EEG signals. The method used a tool of computational intelligence, that is to say an AAN, able to catch the dynamical behavior of the signal and codifying it in a binary string. Such code is comparable with the corresponding codes to/of other mental events.

This way it was possible to identify the chaotic attractors present in the dynamical system represented by the signal and, thanks to these, calculate the content of Integrated Information related to each mental state.

The thesis has been presented by developing the following points.

The concept of consciousness and of Integrated Information has been introduced. Recent studies in the field of neurophysiology brought to the understanding and study of the requirements needed to measure the consciousness, analyzing the composition in quantum terms [94].

The main concept underlying this thesis is that, under controlled stimuli, it is possible to show that similar stimuli correspond to similar responses and different stimuli correspond to different responses, and these responses can be identified and coded.

To elaborate this theory, we studied the brain as a dynamical system and processed signals by means of the chaos theory and a suitable self-organized ANN.

Lastly, we highlighted the processed results with the ITSOM. Moreover, very detailed the different phases of the experiments carried out were described in detail, as well the tools used to record the signals and the choice of the electrodes, the analyzed EEG frequency and the creation and choice of the sensorial and emotive stimuli.

Eventually, the procedure of preprocessing, data registration and the related results have been presented.

The signal analysis with the abovementioned computational method indicated some key points:

In general, there is a correspondence between binary codes and similar mental events, while different mental events have very different codes: to be more precise, it can be noted that there is a constant absence of spurious correspondence between pure colors and images. The most frequent correspondences are between images and written words.

Pure colors are not involved in correspondences as much as we would expect, since they are “easier” perceptions to identify. Moreover, it is observed that a less significant number of correspondences is related to the color red.

The electrode in which correspondences are more frequent is F7, the electrode more involved in cognitive activities. Actually the presence of complex images, not only related to pure perceptions, make a cognitive processing necessary. The electrodes that do not or only partially involve it do not seem apt to generate signals able to recognize similarities between similar images.

Between the two chosen frequencies, the gamma frequency is definitely more selective than the beta one. This is in line with the converging evidence that processes involved in the creation and maintenance of (visual) feature bindings are accompanied by, and systematically related to, neural activity in the gamma band.

A known unifying concept relates the associative principle of neural networks to the

mechanism of temporal binding at high frequencies. It suggests that for each memory stored in an associative network there is a corresponding quasi-stable state of synchronous oscillation at some frequency within the gamma band.

In particular, gamma band power is correlated with visual awareness [95] [96].

The chaotic attractors, isomorphic to the signals and created by the series of winning neurons, are stabilized around 150 epochs and remain stable up until at least 1200 epochs. This allowed us to characterize them and calculate the value of Integrated Information related to each mental state.

We highlighted that the stimulation patterns with cognitive content have a value higher than that of purely perceptive patterns (pure colors). This is completely in line with the Integrated Information Theory.

By continuing the graphic processing of the attractors during the phases, we verified a structural similarity of the attractors of similar cognitive-perceptive content and a different shape in the attractors corresponding to different mental events.

We could try to affirm that the shape of these attractors may constitute a visual counterpart of the “*qualia*”, the elusive qualitative characterization of the conscious states. The present work cannot clearly give a measure about the variation in subjective experience for a given stimulus.

We can affirm that the possibility to computationally encode mental events, based on the dynamical structure of the cerebral signals involved, gives an interesting result that can be confirmed with further experiments.

In particular, the analysis of signals from waking and sleeping patients in the NREM phase is underway with the aim to find a method to distinguish algorithmically the conscious state (waking) from the unconscious state (NREM).

The other result of this thesis is the definition of a method to find the value of Integrated



Information related to real mental states. The ability to measure this value on real cerebral signals opens unexplored perspectives on the possibility to explore conscious and unconscious mental states and add new elements to the understanding of the complicated and fascinating problem of consciousness.

## REFERENCES

- [1] T. Nagel, «What is it like to be a bat? In: Nagel T. *Mortal questions*,» Cambridge: Cambridge University Press, p. p. 165–80, 1979.
- [2] W. James, *The principles of psychology*, New York:: Henry Holt, 1890..
- [3] S.Greenfield, «How might the brain generate consciousness?,» in *From brains to consciousness*, London, In: Rose S, editor, 1998, pp. 210-270.
- [4] G.M. Edelman, G.Tononi, "Consciousness and the integration of information in the brain.," *Consciousness:at the frontiers of neuroscience. Avances in neurology.*, vol. 77, no. 80, p. 245, 1998.
- [5] B.J. Baars, «A cognitive theory of consciousness,,» Cambridge University Press, 1988.
- [6] J. Searle, « The Problem of Consciousness,» *Consciousness and Cognition*, vol. 2, n. 4, pp. 310-319, 1993.
- [7] D. J. Chalmers, «The conscious mind: In Search of a Fundamental Theory,» in Oxford University Press, 1996.
- [8] D. Dennett, *Kinds of Minds: Towards an Understanding of Consciousness*, Basic Books, 1997.
- [9] T. Metzinger, *Neural Correlates Consciousness: Empirical and Conceptual Question*, Mit Press, 2000.
- [10] B. Baars ,N. M. Gage, *Cognition, Brain and Consciousness: An Introduction to Cognitive*, AP, 2007.
- [11] C.S. Sherrington, «The Integrative Action of the Nervous System,» *Brain*, vol. 130, n. 4, pp. 887-894, 2007.
- [12] G.M. Edelman, G.Tononi, «Consciousness and the integration of information in the brain,» *Advances in neurology*, vol. 77, n. 80, p. 245, 1998.
- [13] G.M. Edelman, G. Tononi, *A Universe of Consciousness: How Matter Becomes Imagination*, Basic Books, 2000.
- [14] C. Koch, M. Massimini, M. Boly, G.Tononi, «Neural Correlates of consciousness: progress and problems,» *Neuroscience*, vol. 17, pp. 307-321, 2016.
- [15] G. Tononi, M, Boly, Melanie, M. Massimini, C. Koch, «Integrated information theory: from consciousness to its physical substrate,» *Nature Reviews Neuroscience*. Nature Publishing Group, vol. 17, n. 5, pp. 450-461, 2016.
- [16] M. Boly, M. Massimini, N. Tsuchiya, B.R. Postle, C. Koch, G. Tononi, «Are the Neural Correlates of Consciousness in the Front or in the Back of the Cerebral Cortex?,» *Clinical and Neuroimaging* , vol. 37, n. 40, pp. 9603-9613, 2017.
- [17] C. Shannon, «A Mathematical theory of communication,» *Bell System Technical*

- Journal, vol. 27, pp. 379-423 & 623-656, 1948.
- [18] R. Pizzi, M. Musumeci, «Coding Mental States from EEG Signals and evaluating their Integrated Information Content: a Computational Intelligence Approach,» *International Journal of Circuits, System and Signals Processing*, vol. 11, n. 4464, pp. 464-470, 2017.
- [19] F. Heylighen, «Self-Organization, Emergence and the Architecture of Complexity,» *Proc. European Congress on System Science, AFCET Paris*, pp. 23-32, 1992.
- [20] M. Gell-Mann, «What is Complexity?,» *Complexity* 1, pp. 16-19, 1995.
- [21] R.K. Standish, «On complexity and emergence,» *Complexity Int.*, vol. 9, 2002.
- [22] R. Pizzi, M. Musumeci, *Artificial Neural Networks, Dynamical Systems and Self-Organization*, Create Space, 2017.
- [23] R. Rosen, «Foundations of Mathematical Biology,» *Ac. Press New York*, 1972.
- [24] E. N. Lorenz, , J. Atmos., «Deterministic Nonperiodic Flow,» *Sci.*, Vol. 1 di 220, n. 130, 1963.
- [25] J. Gleick, «Chaos,» *Viking New York*, 1987.
- [26] D. Green, «Emergent behavior in biological systems,» *Complexity Int.*, vol. 1, Aprile 1994.
- [27] D. Kaplan, L. Glass, *Understanding Nonlinear Dynamics,», Springer*, 1995..
- [28] E. Jackson, «Perspectives in Nonlinear Dynamics,» *Cambridge Un. Press*, vol. 1&2, 1989.
- [29] H. Atmanspacher, J. Kurths, «Complexity and Meaning in Nonlinear Dynamical Systems,» *Open Systems and Information Dynamics*, vol. 1, pp. 269-289, 1992.
- [30] R. Rosen, «Dynamical System Theory in Biology,» *Stability Theory and its applications*, vol. 1, 1970.
- [31] H.O. Peitgen, H. Jurgens, D. Saupe, *Chaos and Fractals. New Frontiers of Science*, Springer, 1992.
- [32] B. Mandelbrot, *The Fractal Geometry of Nature,», New York: Freedman&Co*, 1983.
- [33] E. Ott, «Appendix: Hausdorff Dimension,» *Chaos in Dynamical Systems.*, New York, Cambridge University Press, pp. 100-103, 1993.
- [34] S. S. M. Radzi, V. S. Asirvadam, D. K. Y. Hutapea and S. C. Dass, «Comparison of EEG signals during alert and sleep inertia states using fractal dimension,» in *2018 IEEE 14th International Colloquium on Signal Processing & Its Applications (CSPA)*, Batu Feringghi, Malaysia, 2018.
- [35] W.J. Freeman, «Relation of olfactory EEG on behaviour: time series analysis,» *Behavioural Neuroscience*, vol. 100, 1987.
- [36] W.J. Freeman, J. Pelt and F.H. Lopes da Silva, «Role of Chaotic Dynamics in Neural Plasticity, in: *The Self-organizing Brain: from Growth Cones to Functional Networks*,» (eds) Elsevier, 1994.
- [37] V. Menon, W.J. Freeman, «Spatio-temporal Correlations in Human Gamma Band Electroencephalograms,» *Electroenc. and Clin. Neurophys*, n. 98, pp. 89-102, 1996.
- [38] H.E. Schepers, J. Van Beek, J.B. Basingthwaite, «Four methods to estimate the fractal dimension from self-affine signal,» *IEEE Engineering in Medicine and Biology*, vol. 11, pp. 57-64, 1992.
- [39] P. Grassberger, I. Procaccia, «Measuring the strangeness of a strange attractor,» *Physica D*, vol. 9, pp. 189-208, 1983.
- [40] J. Geffries, «Code Recognition and Set Selection with Neural Network,» *Birkhauser*

Boston, 1991..

- [41] R. Hecht-Nielsen, *Neurocomputing*, Addison Wesley, 1990.
- [42] P. Werbos, *Beyond Regression: New Tools for Prediction and Analysis in the Behavioral Sciences.*, Harvard University: PhD thesis, 1974.
- [43] D. Rumelhart, G.E. Hinton, R.J. Williams, «"Learning representations by back-propagating errors",» *Nature*, vol. 323, n. 6088, pp. 533-536, 1986.
- [44] A. Maren, «Neural Networks for Spatio-temporal Pattern Recognition,» in *Handbook of Neural Computation Applications*, Maren A.J., Harston C.T., Pap R.M., Academic Press, 1991.
- [45] Y. Bengio, P. Frasconi, M. Gori, G. Soda,, «Recurrent Neural Networks for Adaptive Temporal Processing,» in *Proc. Neural Nets WIRN Vietri199*, Salerno, 1993.
- [46] F. Pineda, «Generalization of Backpropagation to recurrent and Higher order Neural Networks,» *Physical Review Letters*,, n. 18, pp. 2229-2232, 1987.
- [47] T. Catfolis, «Method for improving the real-time recurrent learning algorithm,» *Neural Networks*, vol. 6, pp. 807-821, 1993.
- [48] K. Funahashi, Y. Nakamura, «Approximation of Dynamical Systems by Continuous Time Recurrent Neural Networks,» *Neural Networks*, vol. 6, 1993.
- [49] M.K. Sundareshan , «Equilibrium Characterization of Dynamical Neural Networks and a Systematic Synthesis Procedure for Associative Memories,» *IEEE Trans. on Neural Networks*, vol. 7, n. 5, Sept. 1991.
- [50] K.S Narendra, K. Parthasarathy, «Gradient methods for the optimization of dynamical systems using neural networks,» *IEEE Trans. on Neural Networks*, n. 2, pp. 252-262,, March 1991.
- [51] R.J. Williams, D. Zipser , «A learning algorithm for continually running fully recurrent neural network,» *Neural Computation*, pp. 270-280, 1989.
- [52] R.J. Williams, J. Peng, «An efficient gradient-based algorithm for on-line training of recurrent network trajectories.,» *Neural Comp*, vol. 2, n. 4, pp. 490-501, 1990.
- [53] R. Grossberg, G.A. Carpenter,, « Self-organization Neural Network Architectures for Real-Time Adaptive Pattern Recognition,,» in: Zometzer S.F. ed., *An Introduction to Neural and Electronic Networks*, Academic Press, 1990.
- [54] G. A. Carpenter, S. Grossberg , J.H Reynolds, «Supervised real-time learning and classification of nonstationary data by a self-organizing neural network,» *Neural Networks*, vol. 4, n. 5, p. 565, 1991.
- [55] M.A. Cohen, S. Grossberg, D. Stork, «Recent Developments in a Neural Model of Real-Time Speech Analysis and Synthesis,» *IEEE First International Conf on Neural Networks*, vol. 4, 1987.
- [56] T. Kohonen, «Self-Organisation and Association Memory,» Springer Verlag, 1983.
- [57] J. Ormrod, *Human Learning*, 3rd edition, Upper Saddle River; Prentice-Hall, NJ, 1999.
- [58] A. Gruart, R. Leal-Campanario, J.C. López-Ramos, J. M. Delgado-García, «Functional basis of associative learning and its relationships with long-term potentiation evoked in the involved neural circuits: Lessons from studies in behaving mammals.,» *Neurobiology of Learning and Memory Elsevier*, n. 124, pp. 3-18, 2015.
- [59] A. Tierney, «The evolution of learned and innate behavior: Contributions from genetics and neurobiology to a theory of behavioral evolution,» *Animal Learning & Behavior*, vol. 14, n. 4, p. 339-348, 1986.

- [60] R.P. Keeling, J. Stevens Dickson, T. Avery , «Biological Bases for Learning and Development Across the Lifespan,» In London M. (Ed.) *The Oxford Handbook of Lifelong Learning* New York: Oxford University Press, pp. 40-51, 2011.
- [61] J. Willis, Bloomington, Solution Tree, «Current Impact of Neuroscience on Teaching and Learning,» *Mind, Brain, Education: Neuroscience Implications for the Classroom*, pp. 45-66, 2010.
- [62] S.L. Willis, K.W. Schaie, M. Martin , *Cognitive Plasticity*, In Bengtson *Handbook of Theories of Aging*, New York: Springer, 2009.
- [63] R. Pizzi, G. Cino, F. Gelain, D. Rossetti, A. Vescovi,, «“Learning in human neural networks on microelectrode arrays”», *Biosystems*, pp. 1-15, 2007.
- [64] R.Pizzi , D.Rossetti, G.Cino, D. Marino, A. Vescovi, W. Baer, «A cultured human neural network operates a robotic actuator.», *BIOSYSTEMS*, vol. 95, pp. 137-144, 2009.
- [65] H. Ritter, K. Schulten , «On the Stationary State of Kohonen's Self-Organizing Sensory Mapping,» *Biological Cybernetics*, n. 54., pp. 99-106, 1986.
- [66] H. Ritter, K. Obermayer, K.Schulten, J. Rubner, *Self-Organizing Maps and Adaptive Filters Models of Neural Network*, E. Domany Springer, 1993.
- [67] T. Kohonen, «Physiological Interpretation of the Self-Organizing Map Algorithm,» *Neural Networks*, vol. 6, pp. 895-905, 1993.
- [68] B. Ermentrout, «Complex Dynamics in WTA Neural Networks with slow inhibition,» *Neural Networks*, vol. 5, 1992.
- [69] S. Amari, «Dynamical stability of Formation of Cortical Maps,» *Dynamic Interaction in Neural Networks: Models and Data*, 1988.
- [70] C.T. Dickson, G. Biella and M. De Curtis, «Evidence for spatial modules mediated by temporal synchronization of carbachol-induced gamma rhythm in medial entorhinal cortex,» *J Neurosci*, n. 20, pp. 7846-7854, 2000.
- [71] J.J. Chrobak, G. Buzsaki, «Gamma oscillations in the entorhinal cortex of the freely behaving rat.,» *J Neurosci*, pp. 388-398, 1998.
- [72] M. Joliot, U.Ribary & R. Llinas, «Human oscillatory brain activity near 40 Hz coexists with cognitive temporal binding,» *Proc. Natl. Acad. Sci USA* 91, pp. 11748-11751, 1994.
- [73] W.H.R. Mitner, C.Braun , M. Arnold ,H. Witte and E. Taub, «Coherence of Gammaband EEG Activity as a Basis for Associative Learning,» *Nature*,, n. 397, pp. 434-436, 1999.
- [74] Rodriguez E., George N., Lachaux J.P., Martinerie J., Renault B. and Varela F.J.,, «Perception's Shadow: Long-distance Synchronization of Human Brain Activity,» *Nature*, n. 397, pp. 430-433, 1999.
- [75] F.J. Varela, «Resonant cell assemblies: a new approach to cognitive function and neuronal synchrony,» vol. 28, pp. 81-95, 1995.
- [76] R. Pizzi, M. de Curtis, C. Dickson, «Evidence of Chaotic Attractors in Cortical Fast Oscillations Tested by an Artificial Neural Network,» in *Proc. WILF2001*, Springer Verlag, Milano, maggio 2001.
- [77] S. K. Nayak , A. Bit , A. Dey , B. Mohapatra, K. Pal, «A Review on the Nonlinear Dynamical System Analysis of Electrocardiogram Signal,» *Journal of Healthcare Engineering*, n. 6920420, pp. 1-19, 2018.
- [78] EMOTIV, Inc., «<https://www.emotiv.com>,» 2011 [Online]. Available: <https://www.emotiv.com>.
- [79] MATLAB, «MATLAB and Statistics Toolbox Release 2012a,» The MathWorks, Natick,

MA.

- [80] J. W. Britton, C. F. Lauren, J. L. Hopp, MD, P. Korb, M. Z. Koubeissi, W. E. Lievens, E. M. Pestana-Knight and Erik K. St. Louis, *Electroencephalography (EEG): An Introductory Text and Atlas of Normal and Abnormal Findings in Adults, Children, and Infants* Chicago, Erik K. St. Louis, MD and Lauren C., 2016.
- [81] E.D. Adrian, «Olfactory reactions in the brain of the hedgehog,» *The Journal Physiology*, vol. 100, n. 4, pp. 459-473, 1942.
- [82] W.J. Freeman, *Neurodynamics: An Exploration in mesoscopic brain dynamicals*, Springer, 2000.
- [83] J.D. Green, A. Arduini, «Hippocampal Electrical activity in aUR,» *Journal of Neurophysiology*, pp. 533-557, 1954.
- [84] C. Pantev, T. Elbert, B. Lütkenhöner, *Oscillatory Event-Related Brain Dynamics.*, New York, 1994.
- [85] R. Eckhorn, R. Bauer, W. Jordan, M. Brosch, W. Kruse, M. Munk, H. J. Reitboeck, «Coherent oscillations: A mechanism of feature linking in the visual cortex? Multiple electrode and correlation analyses in the cat. *Biological Cybernetics*,» *Biological Cybernetics*, vol. 60, n. 2, pp. 121-130, 1998.
- [86] C.M. Gray, W. Singer, «Stimulus-specific neuronal oscillations in orientation columns of cat visual cortex,» pp. 1698-702, 1989.
- [87] A.K. Engel, P. Fries, P.R. Roelfsema, P. König, W. Singer, «Temporal binding, binocular rivalry, and consciousness,» *Conscious Cogn*, vol. 8, pp. 128-151, 1999.
- [88] F. Crick, C. Koch, «A framework for consciousness,» *Nat Neurosci.*, vol. 6, n. 2, pp. 119-126, 2003.
- [89] D. Balduzzi, G. Tononi, «Integrated information in discrete dynamical systems: motivation and theoretical framework,» *Plos Comput. Biol*, vol. 4, n. 100091, 2008.
- [90] G. Tononi, «Consciousness as Integrated Information: a Provisional Manifesto,» *Bio Bull*, vol. 215, pp. 216-242, 2008.
- [91] G. Tononi, «Integrate information theory of consciousness: an updated account,» *Archives Italiennes de biologie*, vol. 150, n. 4, pp. 293-329, 2012.
- [92] G. Tononi, «Integrated Information Theory» [Online]. Available: <http://integratedinformationtheory.org>.
- [93] M. Oizumi, L. Albantakis, G. Tononi, «From the Phenomenology to the Mechanisms of Consciousness: Integrated information Theory 3.0,» *PLOS Comput. Biol.*, vol. 10, n. 5, p. e1003588, 2014.
- [94] G. Vitiello, *My double unveiled: The dissipative quantum model of the brain*, John Benjamins Publishing, 2001.
- [95] A. Engel, W. Singer, «Temporal binding and the neural correlates of sensory awareness,» *Trends Cogn Sci*, vol. 5, pp. 16-25, 2001.
- [96] Q. Luo, D. Mitchell, X. Cheng, K. Mondillo, D. McCaffrey, T. Holroyd, J. Blair, «Visual Awareness, Emotion, and Gamma Band Synchronization,» vol. 19, n. 8, pp. 1896-1904, 2009.

## INDEX OF FIGURES

Figure 1-1 Composition of the thalamocortical system	7
Figure 2-1 Typical trajectories in a two dimensional space with two memories and a limit cycle model	29
Figure 2-2 Recurrent network with state feedback	34
Figure 2-3 Narendra Architecture	35
Figure 2-4 Kohonen Self organizing Map	38
Figure 2-5 Rotation of the weight vectors	39
Figure 2-6 Series of the winning neurons in 2-dimensional state space	41
Figure 2-7 ITSOM Architecture	42
Figure 2-8 Entorhinal median cortex signals before and after carbachol administration	47
Figure 2-9 State space attractors before and after carbachol administration	48
Figure 3-1 The EMOTIV EPOC +	52
Figure 3-2 Display of the electrodes contact quality	53
Figure 3-3 EEG Channels	54
Figure 3-4 FFT EEG Band	55
Figure 3-5 Brain Activity Map	56
Figure 3-6 Brain Activity summary	56
Figure 3-7 EPOC Simulink Signal Server	57
Figure 3-8 The Simulink blocks	58
Figure 3-9 3D-Excelvan Glasses	60
Figure 3-10 The first Colors test	67
Figure 3-11 The second Colors Test	69
Figure 4-1 From the Epoc+ manual: Epoc+ parameters	71
Figure 4-2 System representation	73
Figure 4-3 Series of winning neurons of the yellow stimulation on electrode F7	76
Figure 4-4 Snapshot of the weights variation file, indicating the ANN evolution in the time	77
Figure 4-5 List of Z real numbers	77
Figure 4-6 0s and 1s sequence that represents the network dynamic behavior	78
Figure 6-1 Attractor of Yellow	91
Figure 6-2 Attractor of Lemon	91
Figure 6-3 Attractor of Written Green	92
Figure 6-4 Conceptual structure of Yellow	92
Figure 6-5 Conceptual structure of Lemon	93
Figure 6-6 Conceptual structure of written Green	93

## INDEX OF TABLES

Table 1 Types of Simulink blocks with description	59
Table 2 Selected electrodes F7 (frontal Lobe) and T8 (temporal lobe)	63
Table 3 Selected electrodes P7 (parietal Lobe) and O1(occipital Lobe)	64
Table 4 First Colors test	66
Table 5 Second Colors test	68
Table 6 Subjects Data	70
Table 7 Initial parameters for ITSOM	75
Table 8 Optimized ITSOM parameters	79
Table 9 First Colors test: highest correlation between stimuli and electrodes	80
Table 10 Stimulus, Electrode and corresponding binary code: best similarities	81
Table 11 Second Colors test: highest correlation between stimuli and electrodes	82
Table 12 Stimuli, Electrodes and Binary codes of the second Colors test	84
Table 13 Results of the Yellow stimulus	86
Table 14 Results of the Blue stimulus	87
Table 15 Results of the Green stimulus	88
Table 16 Summary of the results	94
Table 17 Integrated Information Calculus	95